



HAL
open science

Flow and fate of silver nanoparticles in small French catchments under different land-uses: The first one-year study

Jialan Wang, Enrica Alasonati, Mickael Tharaud, Alexandre Gelabert, Paola Fiscaro, Marc F. Benedetti

► To cite this version:

Jialan Wang, Enrica Alasonati, Mickael Tharaud, Alexandre Gelabert, Paola Fiscaro, et al.. Flow and fate of silver nanoparticles in small French catchments under different land-uses: The first one-year study. *Water Research*, 2020, 176, pp.115722. 10.1016/j.watres.2020.115722 . hal-02565467

HAL Id: hal-02565467

<https://hal.science/hal-02565467>

Submitted on 6 May 2020

HAL is a multi-disciplinary open access archive for the deposit and dissemination of scientific research documents, whether they are published or not. The documents may come from teaching and research institutions in France or abroad, or from public or private research centers.

L'archive ouverte pluridisciplinaire **HAL**, est destinée au dépôt et à la diffusion de documents scientifiques de niveau recherche, publiés ou non, émanant des établissements d'enseignement et de recherche français ou étrangers, des laboratoires publics ou privés.

1 **Flow and fate of silver nanoparticles in small French catchments under**
2 **different land-uses: The first one-year study**

3
4 Jia-Lan Wang^{1,2}, Enrica Alasonati², Mickaël Tharaud¹, Alexandre Gelabert¹, Paola
5 Fisticaro², Marc F. Benedetti^{1*}

6
7 ¹ Université de Paris, Institut de physique du globe de Paris, CNRS, F-75005 Paris,
8 France.

9 ² Department of Biomedical and Inorganic Chemistry, Laboratoire National de Métro-
10 logie et d'Essais (LNE), 1 rue Gaston Boissier, Paris, 75015 France

11
12
13
14 *Corresponding author

15 Email: benedetti@ipgp.fr (M. F. Benedetti)

16 Phone number: +33 1 83 95 76 95

17

18

19

20

21 **Abstract**

22 This study focused on surface waters from three small creeks, within the Seine River
23 watershed, which are characterized by different land-uses, namely forested, agricultural
24 and urban. Silver nanoparticles (Ag-NPs) in these waters were detected and quantified
25 by single-particle ICPMS during one-year of monthly sampling. Their temporal and
26 spatial variations were investigated. Ag-NPs, in the three types of surface water, were
27 found to range from 1.5×10^7 to 2.3×10^9 particles L^{-1} and from 0.4 to 28.3 ng L^{-1} at
28 number and mass concentrations, respectively. These values are in consistent with the
29 very few previous studies.

30 In addition, the role of factors driving process and potential sources are discussed with
31 correlations between Ag-NPs concentrations and biogeochemical parameters, like dis-
32 solved organic carbon concentration and divalent cations concentrations. For the forest-
33 ed watershed NOM controls the stability (number and mass) of the Ag-NPs as recently
34 observed in the field in lake water in Germany. In the case of the agricultural and urban
35 watersheds major cations such as Ca would control the number and mass of Ag-NPs.
36 Dilution processes are rejected as conductivity and Cl^- ions do not show significant cor-
37 relations with Ag-NPs or other major geochemical parameters. The specific exportation
38 rates of Ag-NPs for artificial, agricultural and forested areas were calculated based on
39 the monthly data for the full year and are equal to 5.5 ± 3.0 , 0.5 ± 0.3 and 0.2 ± 0.2 gy^{-1}
40 km^{-2} , respectively. These data suggest a constant release of Ag-NPs from consumer
41 products into freshwaters in artificial areas, for instance, from textiles, washing ma-
42 chines, domestic tap-water filters, outdoor paints.

43 These first data of Ag-NPs fluxes in surface waters of France enlarge the very limited
44 database of field measurements. Moreover, for the first time, the influence of time, land-
45 use and aquatic geochemistry parameters on Ag-NPs in real natural water samples is

46 reported. It is also helpful to further understand the fate and the process of Ag-NPs in
47 natural waters, as well as to the ecotoxicity studies in real-world environment.

48

49 **Keywords**

50 Silver nanoparticles; surface water; single particle ICPMS; land-use; fate; concentration

51 **1. Introduction**

52 The first report of silver colloids goes back to 130 years ago in 1889 (Lea, 1889). For
53 decades, nanosilver was mostly used under different names (Collargol, Argyrol, and
54 Protargol) in therapeutic treatments (Nowack et al., 2011). More recently, the introduc-
55 tion and rapid development of nanotechnology opened up wider applications of silver
56 nanoparticles, including textiles, cosmetics, food packaging, medical devices, catalysts,
57 electronics, biosensors... Moreover, silver nanoparticles are reported by Vance (Vance,
58 2015) as the most frequently used nanomaterial and found in 435 consumer products
59 (24% of total items). In a more general way, these silver nanoparticles may find their
60 way into natural waters during their life-cycle. Even though wastewater treatment plants
61 (WWTPs) are effective to remove silver nanoparticles, nano-sized silver/silver sulfides
62 were found in the effluent of WWTPs (Wang et al., 2018). For Europe input rate via
63 WWTP residues to soils is estimated 0.37 tons.y^{-1} and 4.7 tons.y^{-1} to large rivers (Wang
64 et al., 2018). In addition to anthropogenic sources, silver nanoparticles could be also
65 naturally formed from the silver ions in the water or in soils as recently reported by
66 Huang et al (2019) for soils and Wimmer et. al. (2018) for fresh waters. Johnson et al.
67 (2005) have estimated for France an input of 11 tons y^{-1} of anthropogenic bulk silver
68 from waste management to surface environments. Official registration in France recent-
69 ly reported 10 kg in 2017 (R-nano: <https://www.r-nano.fr>) that is a very small amount,
70 so we would not expect to see too much engineered nano-Ag in waters. However, using
71 the data of Wang et al. (2018) for Europe and downscaling it to France, using Europe
72 and France populations as the scaling factor, we can also estimate that 27 kg Ag-Nano
73 y^{-1} and $425 \text{ kg Ag-Nano y}^{-1}$ will be delivered to soils and waters, respectively.

74 This extensive spreading of nano-sized silver and the lack of information regarding their
75 long-term effect inevitably cause emerging concerns about their potential risks to aquatic
76 ecosystems and/or humans. Despite a long history of use, more and more studies

77 showed their adverse impacts on aquatic and terrestrial organisms, mammalian cells,
78 and potentially on human health (Bian et al., 2019; Dobrzyńska and Kruszewski, 2014;
79 Gaillet and Rouanet, 2015; Johnston et al., 2010). Musee (Musee, 2010) modeled their
80 possible toxicity to the aquatic ecosystems of the city of Johannesburg, with a risk quo-
81 tient (defined as the ratio of the estimated environmental exposure to the predicted no-
82 effect concentration) mostly > 1 .

83 The detection and quantification of nanosized silver, from different sources ranging
84 from engineered and incidental to natural ones in the environment and named from here
85 and after Ag-NPs, is however quite limited because of their expected low concentrations
86 and the biogeochemical complexity of aquatic ecosystems. To circumvent this limita-
87 tion, material flow analysis models have been developed to predict environmental con-
88 centrations since 2007 (Boxall et al., 2007). The modeled concentrations of Ag-NPs in
89 surface waters vary significantly, from 0.008 to 619 ng L⁻¹, depending on modeling pa-
90 rameters and studied sites (Dumont et al., 2015; Good et al., 2016; Gottschalk et al.,
91 2015; Mueller and Nowack, 2008; Musee, 2010; O'Brien and Cummins, 2010; Silva et
92 al., 2011; Sun et al., 2016). However, these predictions are currently not validated due
93 to the lack of field measurements in aquatic environments which also limits the further
94 advancement of modeling in other domains, such as their fate and toxicology in com-
95 plex ecosystems. There is thus an urgent need for frequent and robust measurements of
96 Ag-NPs concentrations on fluxes in continental surface waters.

97 A first issue is that to date, only a limited number of studies are available on the quanti-
98 fication of Ag-NPs in freshwaters. Some of them confirmed the presence of colloidal
99 (Wen et al., 1997) and more recently nano silver in wastewater effluent and river water
100 (Mitrano et al., 2012; Peters et al., 2018; Yang and Wang, 2016). However, most studies
101 either focus on one sampling site or several sites along the same river for which a single

102 sampling is performed. Moreover, those studies do not try to relate changes in concen-
103 tration or size of Ag-NPs to bulk geochemical parameters (i.e., pH, dissolved organic
104 carbon concentration, ionic strength, redox...) of the aquatic ecosystems. As for any
105 other type of natural colloids (Benedetti et al., 2003b; Ilina et al., 2016), it is also ex-
106 pected that the Ag-NPs flux will vary along the river and with the hydrological and cli-
107 matic variations during the year. This knowledge is critical to build better material flow
108 analysis models that can take into account such variations if they exist, and give outputs
109 that can be compared to real field data like the one collected in this work.

110 The second issue is the identification, in the field, of the mechanisms and sources that
111 could account for the variations of measured concentrations and fluxes of Ag-NPs
112 among different type of waters. Indeed, most of the processes reported in literature are
113 determined from laboratory experiments (Shevlin et al., 2018) or small scale column
114 experiments to understand the fate of Ag-NPs in soils solutions and their migration to-
115 wards continental waters (Yang et al., 2014). This vast literature reports that organic
116 matter (OM), pH, ionic strength, redox conditions and the concentration of charged cat-
117 ions (i.e., Ca^{2+} , Al^{3+} ...) are critical parameters that will control the number and size of
118 Ag-NPs in such designed experiments. Only recently, Wimmer et al. (2018) showed
119 that in field, in lake water, OM promoted the formation of AgNPs. These factors were
120 also shown to be important for the fate of trace metals and contaminants in a watershed
121 under a high anthropogenic pressure like the Seine River (Bonnot et al., 2016). The di-
122 rect evidence, from field data, of the role played by such drivers is still missing. It is
123 therefore important to explore how they will be effectively related to changes in concen-
124 tration, size and flux of Ag-NPs in river watersheds.

125 The third issue, generally addressed in material flow analysis models but not in today
126 published field studies, is the impact of the land-use within a watershed. For instance,

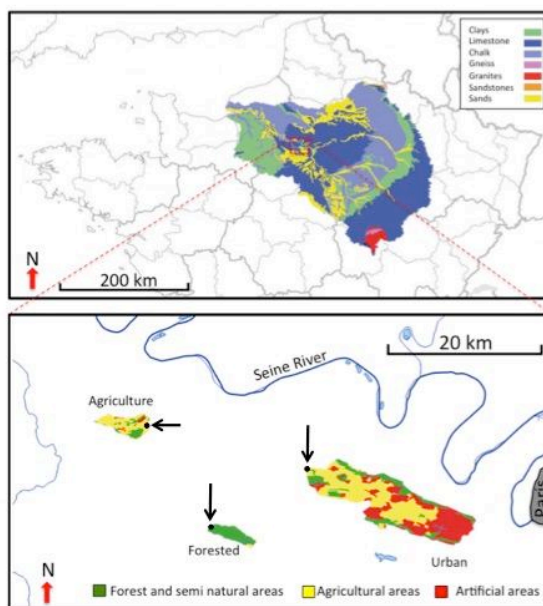
127 for the whole Seine River watershed, an increase in trace metal concentrations from
128 « pristine » headwaters to heavily impacted urban-waters was reported (Chen et al.,
129 2014; Grosbois et al., 2006; Horowitz et al., 1999), with a significant impact of Paris
130 conurbation due to wastewater treatment plants and combined sewer overflow inputs
131 (Estebe, A., Mouchel, J.M. Thévenot, 1998; Garban B, Ollivon D, Carru AM, 1996). In
132 addition, a recent field monitoring of Ag-NPs was conducted on Meuse and Ijssel wa-
133 tersheds which are characterized by different land-uses (Peters et al., 2018). Based on
134 the measured concentrations of Ag-NPs from this study, a first order estimation of the
135 Ag-NPs normalized export-rates can be calculated using an annual average discharge
136 rate and watershed area (source Wikipedia, 2018). We calculated the export-rates nor-
137 malized per km² or per capita and they are equal to 0.3 g km⁻²y⁻¹ (1 mg Ag-NPs capita⁻¹
138 y⁻¹) and 2.0 g km⁻²y⁻¹ (6 mg Ag-NPs capita⁻¹y⁻¹), for the Meuse and Ijssel rivers, re-
139 spectively. Using only the 10 kg of nano-engineered /year declared in the R-nano data-
140 base gives a rate of release equal to 0.15 mg Ag-NPs/y/capita for France”. Potential
141 explanations for such differences in two rivers are: their different processes governing
142 the fate of the NPs along the rivers’ course, their differences in soils nature and in com-
143 positions, and may be the most importantly, their differences in land-use. For instance,
144 the Meuse basin is comprised by croplands (39%), forests (29%), pastures (18%) and
145 built up areas (12%) by the end of the 20th century (Lambert et al., 2017); while rural
146 areas characterize the Ijssel watershed with intensive agricultural dominating with
147 croplands covering 70% of the basin (Verwijmeren and Wiering, 2007). Putting aside
148 the obvious effect of the land-use for the contaminants and Ag-NPs sources mobiliza-
149 tion, one can wonder to what extent are the normalized fluxes of Ag-NPs governed by
150 the land-use, or if these fluxes are only regulated by the above mentioned biogeochemi-
151 cal drivers. The answers to these questions will help to better constrain the hypothesis
152 made in material flow analysis models. They will also provide an accurate range of Ag-

153 NPs environmental concentrations in combination with realistic biogeochemical param-
154 eter values to be tested in future studies on Ag-NPs toxicity toward aquatic fauna.

155 To address those issues, the best approach is to sample waters from low to heavily hu-
156 man-impacted territories and to precisely assess the seasonal dynamics of Ag-NPs under
157 such different land-uses. The present study relies on concentration analysis for the dis-
158 solved (< 1 kDa) and nano-particulate silver in three characteristic sub-basins (i.e., for-
159 ested, agricultural, and urban), selected in a previous study on the identification of trace
160 element geochemical background values in the Seine River watershed (Bonnot et al.,
161 2016). Small size sub-watersheds (< 120 km²) were chosen as the water samples will be
162 prone to rapid modifications of their biogeochemical parameters as a function of hydro-
163 climatic and land-use changes, in order to identify their role on the Ag-NPs concentra-
164 tion and fate and to inter-compare export rates specific to these three land-uses.

165 2. Materials and Methods

166 2.1 Sampling sites and protocol



167

168 Figure 1: Characteristics of three sampling catchments (Agriculture, Forested and Urban) in the Seine River watershed of France.
169 Data to built the maps are from Bonnot et al, (2016). Arrows pointing to the sampling location, exact coordinates are given in the
170 supplementary material.

171 The three sampling sites are located on the west of Paris. Their lithology and land uses,
172 composed of artificial surfaces, agricultural areas and natural areas, are given in Fig. 1.
173 Detailed information on the watersheds area, distribution of land uses and discharge
174 rates as measured during this study are given in Table S1. A snapshot of the water geo-
175 chemistry was obtained by grab sampling of the three creek waters taken each month or
176 each two months from October 2016 to December 2017 for Ag-NPs detection, using 1 L
177 polyethylene containers. Before field sampling, the containers were previously washed
178 with 1 N HCl for 2 days, then rinsed three times with MQ water in the laboratory. On
179 each sampling site, one 1 L bottle was placed horizontally at the surface (about 10 cm)
180 of creek until filled by water and it was done within 5 to 10 seconds depending of the
181 flow rate. For the urban watershed, the water was collected from a bridge with a bucket
182 and the 1L bottle filled directly with the bucket in less than 5 seconds.

183 To evaluate the sampling effect, three additional samplings were performed for each
184 sampling site during three field missions. Sampling replicates were individually ana-
185 lyzed to evaluate the contribution of sampling to the overall uncertainty. The sampling
186 effect was evaluated by performing ANOVA test for water sampling replicates, and was
187 not significant.

188 The pH, dissolved oxygen and conductivity were measured in the field using Multi
189 3410 Multiparameter Meter. The sensors and electrodes were calibrated before field
190 measurements in the lab and the calibration verified in the field prior to measurements.
191 Various sub-aliquots were filtered in the field through 0.22 μm (cellulose acetate) for
192 analysis of the dissolved anions (non-acidified) and cations (acidified). Triplicate sub-
193 samples were acidified with 65% HNO_3 for trace elements and rare earth elements anal-
194 ysis. Glass vials previously washed with acid, rinsed and pyrolyzed at 500°C were used
195 to store samples for the analysis of dissolved organic carbon (DOC) obtained from an-
196 other aliquot filtered through 0.7 μm glass microfiber filters, and acidified with 85%

197 H₃PO₄. All containers and materials used for sampling were rinsed three times with riv-
198 er waters in the field before collection.

199 Unacidified, unfiltered sub-samples were immediately analyzed back to laboratory for
200 alkalinity determination and all the others above-mentioned samples were stocked at
201 4°C prior to analysis. The alkalinity was measured by titration with 10⁻² mol L⁻¹ HCl
202 (Titrand 809, Metrohm). The DOC was analyzed with a Total Organic Carbon Ana-
203 lyzer (TOC-L, Shimadzu). The anions were quantified with ion chromatography (Dionex
204 ICS 1100, Thermo Scientific®). The cations were analyzed with an ICP-AES (iCAP
205 6200 Series, Thermo Scientific®). So-called dissolved (i.e., < 0.22 µm and < 1 kDa)
206 trace element concentrations were determined with a HR-ICP-MS (Element II, Thermo
207 Scientific®) and the raw data were treated with uFREASI software (Tharaud et al.,
208 2015). Immediately after field sampling, in the laboratory, an aliquot (500 mL) of the
209 bulk 1 L sample, taken for Ag-NPs analysis, was ultra-filtered through 1 kDa (regener-
210 ated cellulose) in order to remove all the particles present in waters to get access to the
211 fraction of free Ag ions and Ag bound to organic matter or associated to nanoparticles
212 smaller than a few nanometers (≤ 1.3 nm) (Guo and Santschi, 2007). This ultra-filtrate
213 was further used as the matrix to prepare all standards and solutions for sp-ICPMS
214 analysis. It aims at conserving the same environment of Ag-NPs in waters and avoiding
215 matrix effect during measurement.

216 **Digestion of bulk water**

217 Additionally in 2019, the total silver was quantified after acid digestion in 9 samples,
218 which came from the urban watershed. A sub sample of 10 mL was taken for total silver
219 analysis in triplicates and mineralized with a mixture of 3 concentrated acids (3 mL
220 HCl, 1 mL HNO₃ and 0.5 mL HF) in a PFA closed vessel and heated for 24 H at 105
221 °C. After the digestion the mixture was evaporated at 85 °C to dryness. The residue was
222 then dissolved in 10 mL of 2% HNO₃. Blanks were run at the same time in triplicates

223 and PFA vessels were cleaned with a concentrated HNO₃ at 120 °C before use and
224 rinsed 3 times with MQ water.

225

226 **2.2 Single-particles ICPMS (sp-ICPMS) measurements of Ag-NPs**

227 **Instrumental parameter and standard preparation**

228 A high resolution ICPMS - Thermo Scientific ELEMENT II was used for Ag-NPs
229 measurements in this study. It was joined with a quartz cyclonic spray chamber and a
230 PFA MicroFlow nebulizer. The peristaltic pump rate was set at 12 rpm generating a
231 sample uptake flow of 0.2 mL min⁻¹. Certified reference material Au nanoparticles of 60
232 nm (RM8013, NIST) was used to determine sample loss during sample uptake (*ca.*
233 transport efficiency). The Au-NP stock suspension was diluted 2.5 x 10⁵ times in the
234 ultra-filtered matrix to achieve a proper particle concentration for sp-ICPMS measure-
235 ments and avoid NPs coincidence at milli-second dwell-time. Dissolved calibration
236 curves (Au: 50 to 5000 ng L⁻¹; Ag: 50 to 1000 ng L⁻¹) were prepared in the ultra-filtered
237 matrix to determine the element sensitivity in the same matrix as the water samples and
238 thus prevent matrix effect. The analysis of Ag-NPs in river waters was carried out with
239 1 ms dwell time, and 1 ms settling time (Tharaud et al., 2017). 10 000 data points were
240 acquired and the isotope ¹⁰⁷Ag and ¹⁹⁷Au were measured in low resolution mode and
241 each measurement was performed in triplicate which allows to calculate means and
242 standard deviations. The dilution of the natural water samples was unnecessary consid-
243 ering the expected low concentrations in natural waters. All suspensions and solutions
244 were freshly prepared, with the minimum delay between sampling and analysis.

245 **Data processing**

246 According to the literature, the transport efficiency (TE) is needed to determine the con-
247 centration and size of Ag-NPs in river waters and can be obtained by three methods,
248 based on 1) waste collection, 2) particle size, and 3) particle frequency (Pace et al.,

249 2011). Here, the second method is selected since the reference material used in this
250 study is better certified for the particle size than the particle concentration. Taking into
251 account the matrix effect, TE was determined independently for each type of river wa-
252 ter. The calculation method and the formula of TE are detailed in the supplementary
253 materials.

254 Before data processing can be performed, NPs must be correctly distinguished from the
255 dissolved background. Different methods exist to determine the threshold between dis-
256 solved and particulate fractions, such as average plus 3σ (Pace et al., 2012), iterative
257 algorithms with 3σ (Tuoriniemi and Hassellöv, 2012) or simply by using the first mini-
258 mum as the boundary between dissolved fraction and NPs (Montaño et al., 2014). How-
259 ever, for the size range expected for Ag-NPs (Peters et al., 2018), those approaches
260 could lead to a large number of false negatives during NPs counting (i.e., underestima-
261 tion of the representative number of NPs events). Instead, we used in this study another
262 approach to prevent such artifacts: the subtraction method. It is analogous to the
263 deconvolution method (Cornelis and Hassellöv, 2014), but uses the ultra-filtered natural
264 waters as the blank. Because the ultra-filtrate was supposed to best represent the realis-
265 tic dissolved background in case of natural water samples. Basically, the histogram of
266 frequency vs intensity of the ultra-filtrate through 1 kDa is subtracted from that of the
267 raw water sample using the same bin-width (same range of intensity for each bin of both
268 histograms). The resulting histogram is then used to calculate the concentration and size
269 of Ag-NPs. Calculations of particle-number concentration from the signal frequency,
270 and of particle size from the signal intensity, are well-described in literature. Here we
271 used the procedure developed by Pace and co-workers (Pace et al., 2011).

272 **3. Results and Discussion**

273 **3.1 Ag-NPs concentrations in three waters**

274 Table 1. Concentration and size of Ag-NPs measured in surface waters from the literature and present study measurements. PEC:
 275 Predicted Environmental Concentrations in surface water values taken from Peters et al., 2018. *10% most exposed rivers according
 276 to Dumont et al., 2015. n.g. not given; n.a. not analyzed.
 277

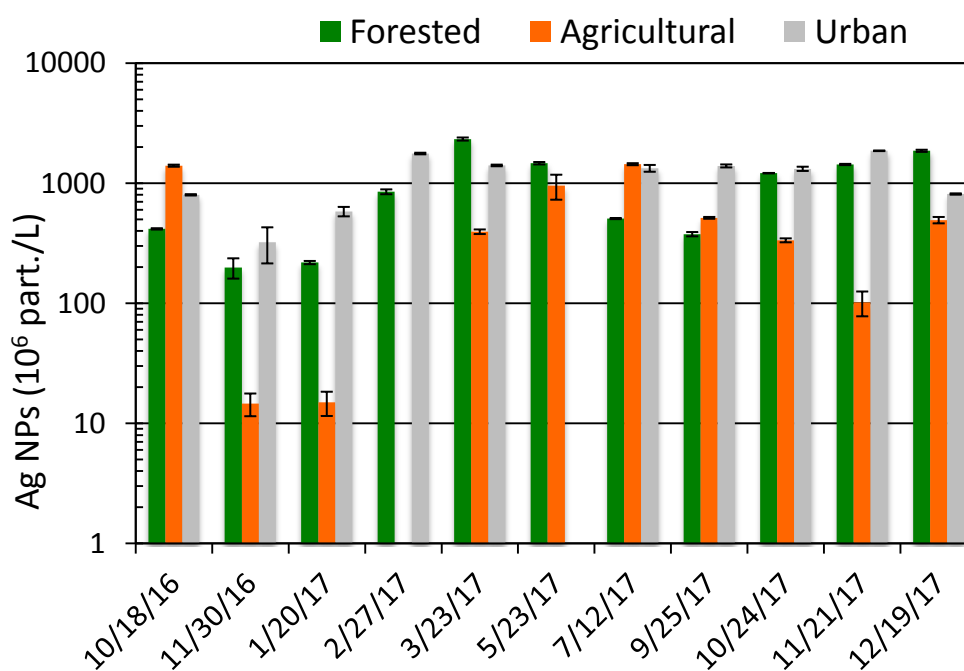
	Range / Average 10 ⁸ particle L ⁻¹	Range / Average ng L ⁻¹	Size nm	References
PEC compilation	n.g.	0.04 – 619	n.a.	In Peters et al., 2018
PEC (Europe surface waters)	n.g.	0.002 – 2.3 / 0.3*	n.a.	Dumont et al., 2015
Rivers of Texas	n.a.	0.01- 62 ^a / n.g.	n.a.	Wen et al., 1997
China (Chendian Lake and Guiyu River)	0.4 – 0.7 / n.g.	n.a.	n.g.	Yang et al., 2016
Netherlands (Ijssel and Meuse Rivers)	0.05 – 0.35 / 0.08	0.3 – 2.5 / 0.8	15	Peters et al., 2018
Forested water	2 – 23 / 10	0.8 – 14 / 5	< LOD	This study
Agricultural water	0.1 – 14 / 6	0.4 – 19 / 7	10 – 18 / 12	This study
Urban water	3 – 19 / 11	5 – 28 / 12	10 – 20 / 13	This study

278
 279 First of all, Ag-NPs are detected in all waters sampled throughout the year. The concen-
 280 trations range, their average and their size and the results of previous studies are sum-
 281 marized in Table 1. The presence of Ag-NPs can be directly observed by comparing the
 282 signal of raw water and the matrix-blank with all particles removed (i.e., filtrate through
 283 1 kDa) (Fig. S1). Ag-NPs number concentrations range from 1.5 x 10⁷ to 2.3 x 10⁹ par-
 284 ticles L⁻¹, with an average of 9.1 x 10⁸ particles L⁻¹. Their mass concentrations are in the
 285 range of 0.4 - 28.3 ng L⁻¹, with an average of 7.9 ng L⁻¹. Compared with the scare data-
 286 base of Ag-NPs in surface waters (Table 1), the particle number concentrations found
 287 here are in a larger range and the average is 100 times higher than that of Dutch rivers
 288 (Peters et al., 2018). It mostly results from the different data processing approach ap-
 289 plied. The subtraction method in our study allows to better constrain the false negatives,
 290 where the small Ag-NPs are counted as the dissolved background. Regarding the mass
 291 concentration, our results cover the concentration range of the recent study in surface
 292 waters of Netherland. They are in agreement with previous measurements of colloidal
 293 Ag in Texas Rivers. Moreover, from the modeling view, Ag-NPs are expected in sur-

294 face waters between 0.04 to 619 ng L⁻¹ (Table 1). Our measured concentrations are
295 within this global range, but a bit higher than most estimations for Europe (0.002 to 2.3
296 ng L⁻¹) (Dumont and Williams, 2015). However, the existence of naturally occurring
297 Ag-NPs is not included in the concentration estimation by modeling, resulting in an
298 underestimation in that case. Also, for now, the challenges raised by all modeling stud-
299 ies in natural rivers come from the complex transformations undergone by silver nano-
300 particles on one hand, and their interactions with environmental components on the oth-
301 er hand. Thus, the field data obtained here will constitute a strong constraint to better
302 refine the possible control factors in surface waters.

303 Among the three waters in this study, the largest Ag-NPs amount is found in the urban
304 site, with an average concentration of 1.2 x 10⁹ particle L⁻¹ and of 12.3 ng L⁻¹ (Table 1).
305 Ag-NPs mass concentrations in agricultural and forested waters are very close, consid-
306 ering the significant variations measured over the year. However, the forested water has
307 a higher particle-number concentration than the agricultural water. This is mainly as-
308 cribed to their different size populations of Ag-NPs (Table 1). The size might be related
309 to the water geochemistry affecting processes of Ag-NPs in this environment, which is
310 to be discussed in more details in following sections.

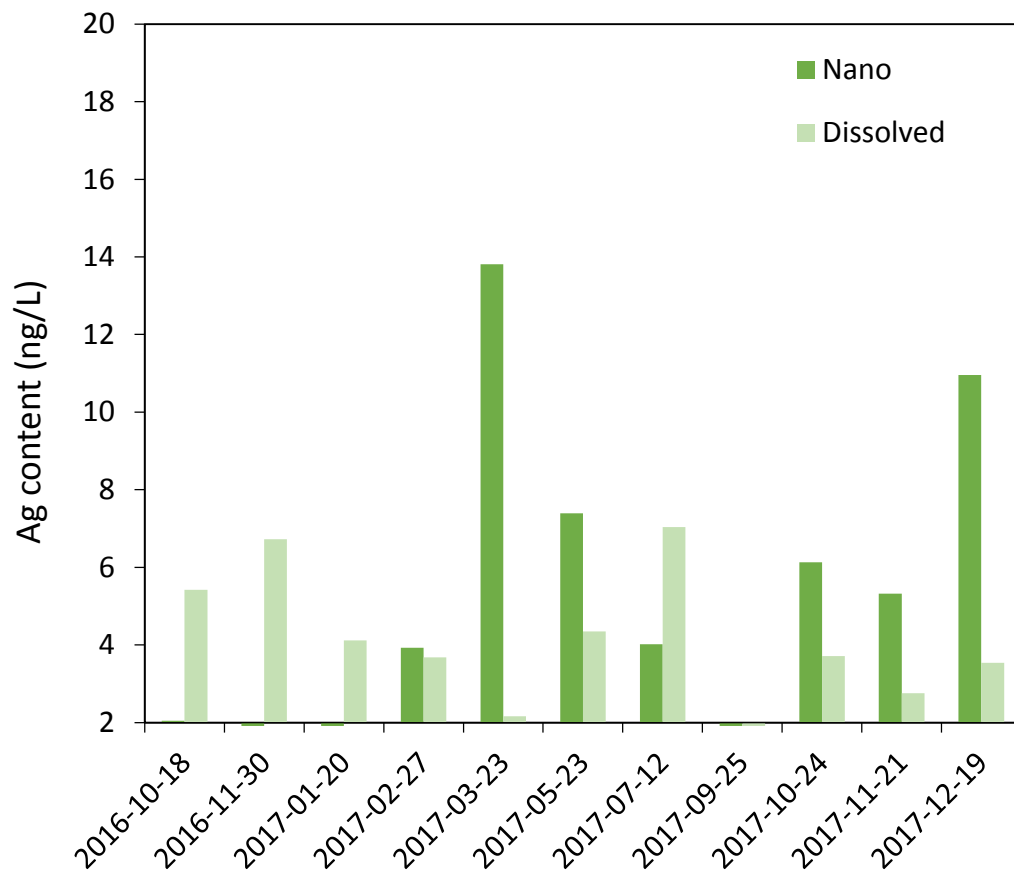
311 Monthly sampling was performed on each catchment to investigate temporal variations
312 of the Ag-NPs concentration over the year. The particle-number concentrations are pre-
313 sented in Fig. 2.



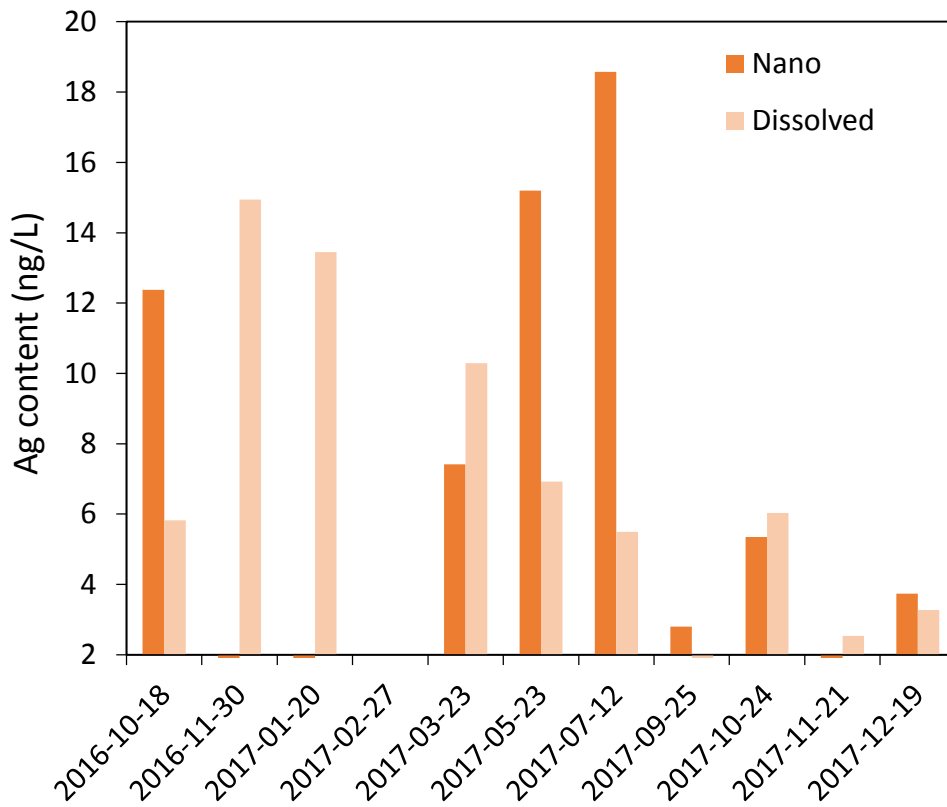
314

315 Figure 2. Flux of Ag-NPs measured in three waters for one-year sampling (except two contaminated cases). Error barres represent
 316 the standard deviation (SD) of three measurements.

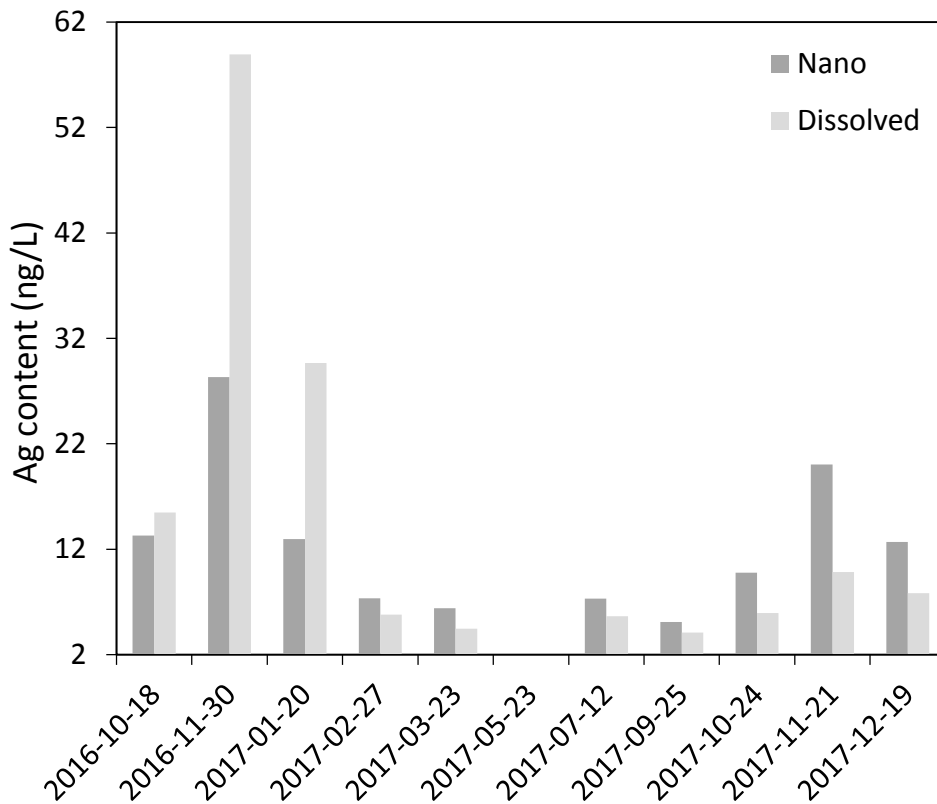
317 It shows that the flux in the urban site is quite constant throughout the whole year, but
 318 the two other sites have larger temporal variations since average annual water flows are:
 319 22 ± 9 L/sec and 51 ± 27 L/sec for the forested and agricultural creeks, respectively.
 320 The larger variations in water flow rates reported for the agricultural and the forested
 321 sites account therefore for the temporal variability showed in Figure 2. Indeed, forested
 322 and agricultural sites, as small watersheds, react very quickly to the climatic and hydro-
 323 logical effects, whereas the urban watershed of greater size has diverse contributions
 324 (mixture of artificial, agricultural and natural areas) and its concentration variation can
 325 thus be slighter over time. Additionally, an increase of Ag-NPs from winter to spring is
 326 observed for forested and agricultural waters. The dissolved silver (< 1 kDa) is also
 327 quantified by sp-ICPMS in order to investigate the speciation of silver in three natural
 328 waters. The signal intensity in counts per second of ultra-filtered samples is converted
 329 into ng L^{-1} , using the dissolved Ag sensitivity calibration curve. Fig. 3 shows the con-
 330 centrations of dissolved and nano Ag in three waters. It should be noted that values un-
 331 der the limit of quantification (2.5 ng L^{-1}) are not discussed here.



332



333



334

335 Figure 3. Mass concentration of nano (dark color) and dissolved (light color) silver measured in three waters. Forested, agricultural
 336 and urban are respectively represented by green, orange and grey bars.

337

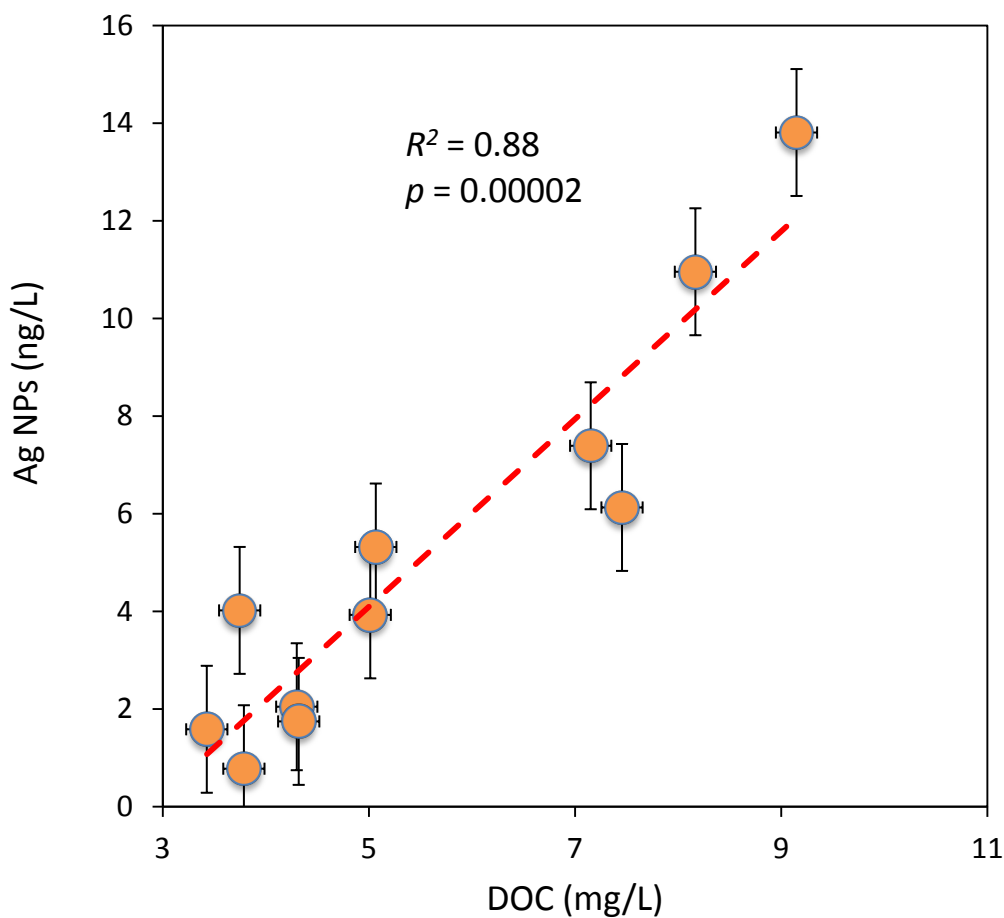
338 For most forested watershed water samples more nano silver is measured than dis-
339 solved, this is in agreement with results of (Delay et al., 2011). showing that NOM sig-
340 nificantly influences the particle size distribution, the stability and the surface properties
341 of Ag-NPs in the aqueous phase preventing it further dissolution, and that in presence
342 NOM, Ag-NPs suspensions are also stable at variable ionic strength, which will facili-
343 tate their transport. In addition it was recently shown that natural organic matter content
344 (i.e. $\leq 10 \text{ mgL}^{-1}$ NOM) in lake water encourage the natural silver-based nanoparticle
345 formation (Wimmer et al., 2018). However, in agricultural and urban waters, the distri-
346 bution changes from one sampling period to another. No conclusion has been made for
347 these two sites, in which the transformation of silver is more complex and may be con-
348 trolled by multiple parameters and processes (size and coating of Ag-NPs, pH, DOC, IS,
349 dissolved oxygen, light irradiation, biofilm...) (Desmau et al., 2018; Shevlin et al.,
350 2018).

351 The total silver quantified in 2019 after acid digestion of the 9 remaining samples, from
352 the urban watershed are given in Table S4. The total amount of Ag is higher than the
353 addition of nanosized and dissolved fractions in almost all urban waters, except the
354 sample of 2016-11-30. This is most probably related to the ageing water samples since
355 those samples were stored in the refrigerator with no prior acidification for two or three
356 years, part of the silver may have been lost to the container wall. Besides, when elimi-
357 nating sample of 2016-11-30, the average of percentage of measured Ag (nano + dis-
358 solved) is equal to 70%. It means that a part of Ag is incorporated in larger particles or
359 aggregates not detected by sp-ICPMS.

360 **3.2 Field mechanisms and the sources accounting for the variations of measured** 361 **concentrations**

362 Correlation between elements and Ag-NPs concentrations (i.e., number or mass) can be
363 interpreted within a mass balance approach or as the identification of driving parameter

364 or process for small watersheds (Benedetti et al., 2003a). All related data in the follow-
365 ing discussion (pH, DOC, conductivity, IS and elements concentrations in the dissolved
366 fraction) are detailed in supplementary material (Table S2 and S3). The correlation be-
367 tween two variants is considered statistically significant *when* $R^2 \geq 0.6$ and p -value \leq
368 0.01. There is a positive correlation between DOC concentrations and Ag-NPs concen-
369 trations in forested water (Fig. 4 and S2).



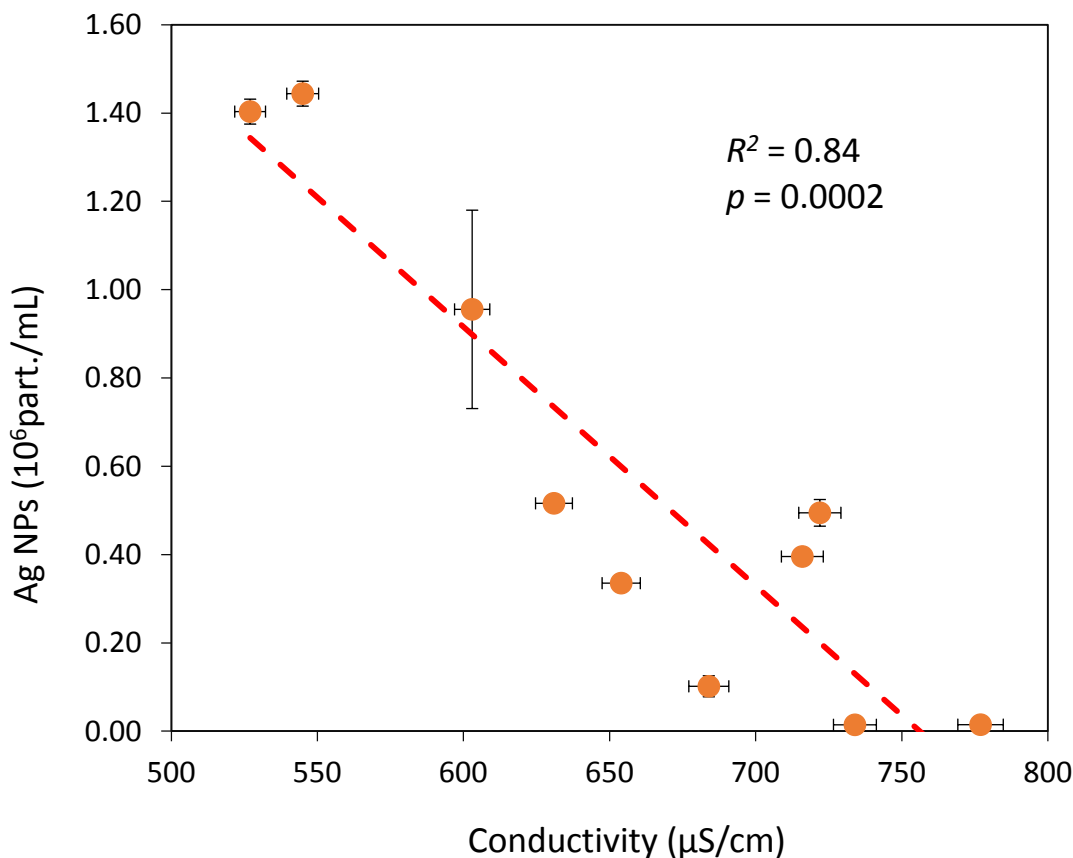
370

371 Figure 4. Mass concentration of Ag-NPs as function as DOC concentration in water samples from the forested watershed.

372

373 This strong correlation reflects the control of the natural organic matter (NOM) on the
374 number and the mass of Ag-NPs. The more NOM, the more Ag-NPs are detected in
375 forested water samples. This trend is explained by two combined effects: stabilization
376 and reduction. The stabilization effect of NOM (humic and fulvic acids) on Ag-NPs has

377 been described in several studies (Topuz and Talinli, 2015; Yu et al., 2018; Zhang and
378 Jiang, 2017; Wimmer et al., 2018; Huang et al., 2019). High NOM concentration inhib-
379 its the dissolution and aggregations of Ag-NPs when released into surface waters, thus
380 making Ag-NPs more persistent in such natural matrices. The formation of Ag-NPs
381 through reduction of Ag^+ by NOM can also lead to the increase of Ag-NPs concentra-
382 tion along with NOM (Akaighe et al., 2011; Sal'nikov et al., 2009; Yin et al., 2012a,
383 Wimmer et al., 2018). As reported in Fig. 3 there is a large reservoir of dissolved Ag,
384 either as free Ag^+ or Ag bound to NOM to justify the potential increase of Ag-NPs by
385 this process. For the agricultural and urban watersheds, no significant trends between
386 DOC and Ag-NPs number or mass concentrations were found. This lack of trend does
387 not mean that similar processes are not at work, but that the smaller range of NOM con-
388 centrations variations $\Delta\text{NOM} = 2.2 \text{ mg L}^{-1}$ and 1.7 mg L^{-1} versus 5.7 mg L^{-1} for agricul-
389 tural and urban versus forested watersheds, respectively, prevented the building of a
390 reliable correlation. Moreover, other potential processes which work more efficiently
391 might be operating in those two watersheds.



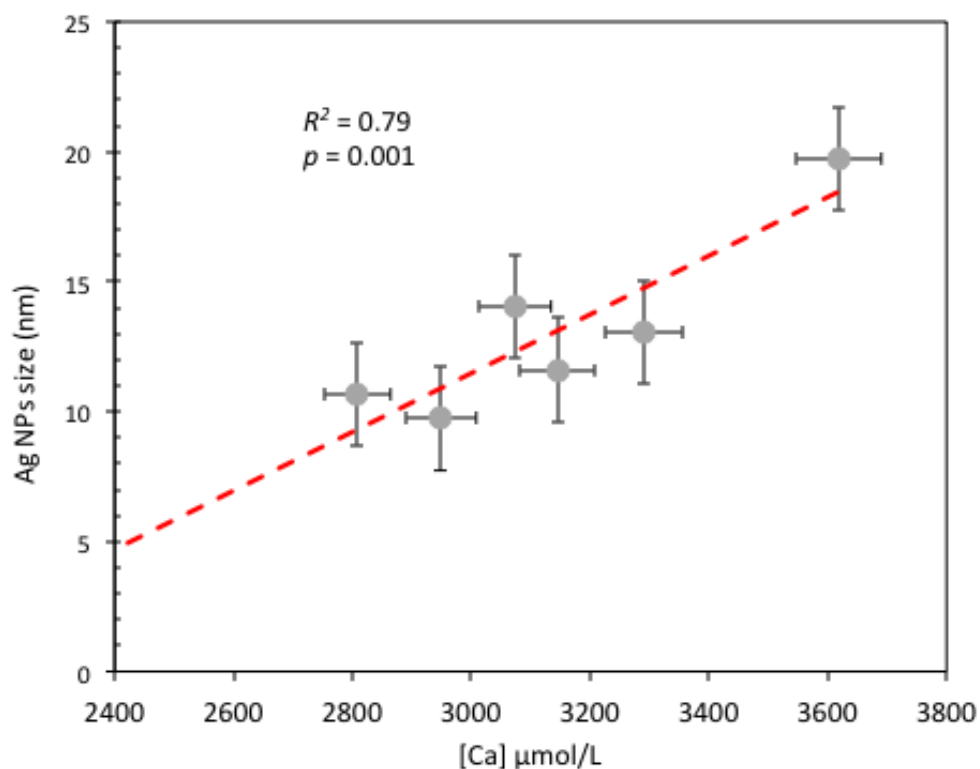
392

393 Figure 5. Number concentration of Ag-NPs as function as conductivity in water samples from the agricultural watershed.

394

395 Indeed, we found that the particle-number concentration and the equivalent size for
 396 sphere of Ag-NPs correlate negatively with conductivity, and positively with Ca con-
 397 centration, in agricultural and urban water samples, respectively (Fig. 5 and 6). This
 398 means that Ag-NPs number concentration decreases with increasing charged ions con-
 399 centration in the aquatic media. The agricultural and urban waters have higher concen-
 400 trations of charged ions, while their average particle size is significantly higher than Ag-
 401 NPs from the forested waters (Table 1). The charge-induced aggregation, and even sed-
 402 imentation, of silver nanoparticles has been reported in simplified natural systems with
 403 the presence of calcium ions (Topuz et al., 2014). These aggregates will interact with
 404 colloids or induce further sedimentation (Labille et al., 2015), thus escape from the top-
 405 layer sampling since the sampling river surfaces are quite small and water column is
 406 shallow (< 0.3 m). In the case of the agricultural water samples the lack of increase in

407 size with Ca^{2+} could be due to fast sedimentation or formation of nanoparticles outside
408 the range of our analytical detection window.

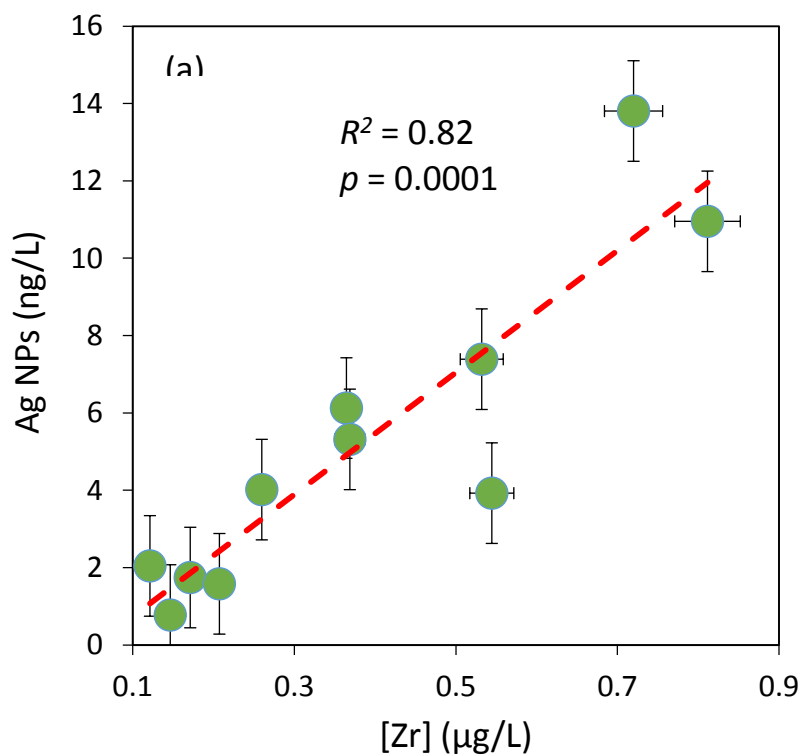


409

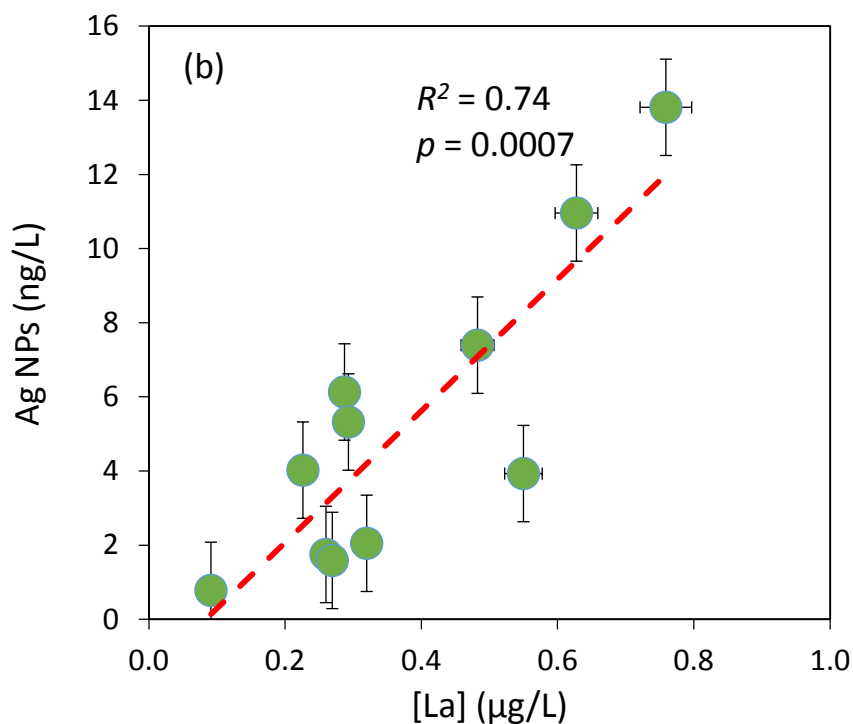
410 Figure 6. Size of Ag-NPs as function as the concentration of dissolved Ca^{2+} ($< 0.22 \mu\text{m}$) in water samples from the urban water-
411 shed.

412 Considering negative correlation between Ag-NPs concentration and conductivity, to-
413 gether with size growing with Ca^{2+} content, we can conclude that in the charge-
414 abundant river, the aggregation or even sedimentation is favorable and the fate is more
415 controlled by charge determining ions such as divalent cations (i.e., Ca^{2+} and Mg^{2+}) or
416 Al^{3+} in extreme conditions with very low pH.

417 Another explanation for this correlation is that the observed changes are related to vari-
418 able inputs of different sources with time for instance the urban watershed is partly cov-
419 ered by agricultural land. But the differences in bulk geochemistry, especially for major
420 ions, are not that large for a single river (Table S3) and cannot totally explain the ob-
421 served trend.



422



423

424 Figure 7. Mass concentration of Ag-NPs as function as the concentration of total Zr and La in water samples from the forested
 425 watershed.

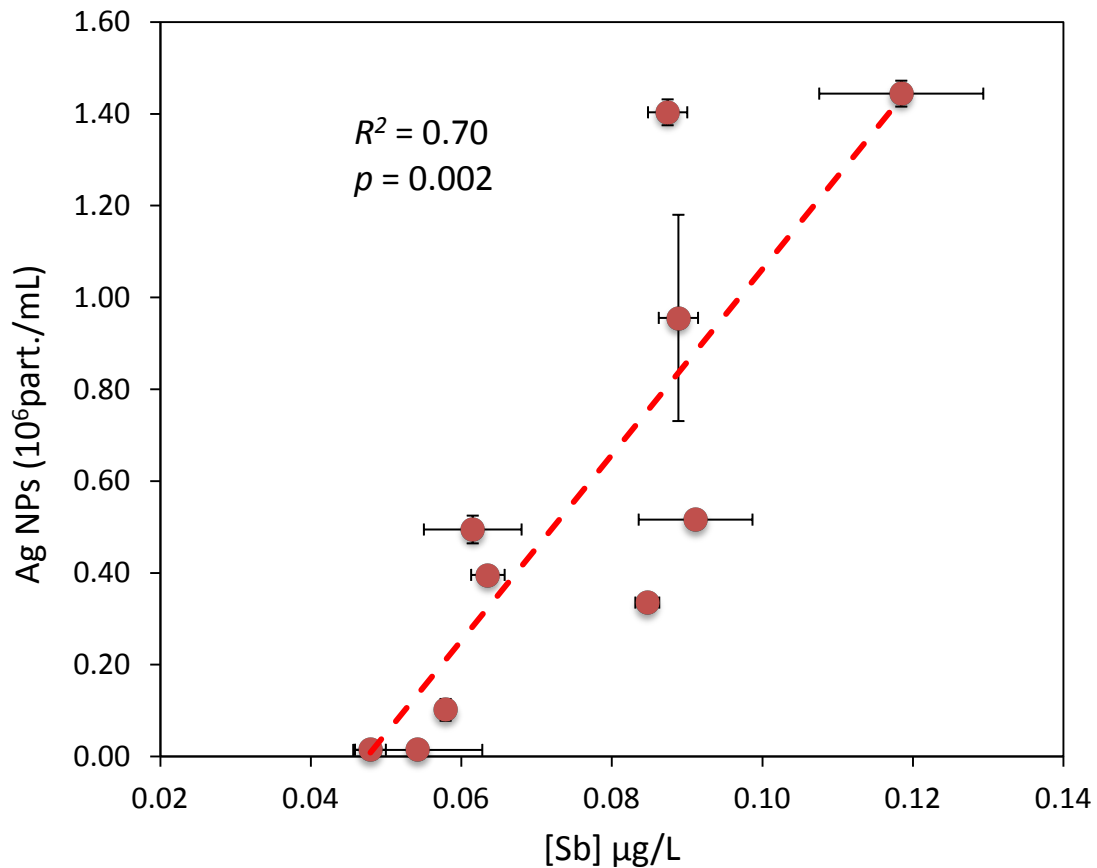
426 However, correlations can also help to identify sources of elements and colloids

427 (Benedetti et al., 2003a). For instance, for the forested site water samples, there is a

428 strong correlation between the Ag-NPs mass concentration and trace elements (Zr, Y,
429 La and Ce) in the fraction $< 0.22 \mu\text{m}$ (two examples are given in Fig. 7 and S3). Zr, is
430 often considered as a geological background indicator because of its limited mobiliza-
431 tion under most environmental conditions (Aja et al., 1995; Hodson, 2002). As for La
432 and Ce, their speciation is generally controlled by natural organic matter (Sonke, 2006),
433 which explains their good correlation with Ag-NPs number and mass concentrations.
434 Moreover, the Ce/La ratio is equal to 1.9 ± 0.1 for all water samples in the forested wa-
435 tershed, this value is equal to the geochemical background value of 1.9 given for French
436 soils and suspended matter sediments (Reimann et al., 2018). Thus, silver nanoparticles
437 in forest water are very likely to be of natural origin. In addition to the natural leaching
438 from bedrock (Qi et al., 2007), other potential pathways of naturally occurring Ag-
439 containing NPs include the reduction of dissolved Ag^+ by natural organic matter
440 (Akaighe et al., 2011; Sal'nikov et al., 2009; Yin et al., 2012a; Wimmer et al., 2018),
441 the oxidation and reduction of macroscale Ag objects (Qi et al., 2007), and biological
442 processes (Klaus et al., 1999; Kroll et al., 2014). Moreover, the stability of Ag-NPs in
443 the environment could be enhanced by surface sulfidation (Levard et al., 2011), via in-
444 teractions with extracellular polymeric substances (EPS) (Kroll et al., 2014; Li et al.,
445 2016) and with NOMs (Topuz and Talinli, 2015; Yu et al., 2018; Zhang and Jiang,
446 2017) present in the natural matrix.

447 Le Pape et al. (2012) identified Antimony (Sb) as a typical anthropogenic element in the
448 Orge river catchment, very close to our sampled watersheds. They concluded that Sb
449 was of anthropogenic origin and carried by organic matter or sulfur containing species.
450 In the agricultural watershed we have a good correlation between Sb and Ag-NPs num-
451 ber concentration (Fig. 8). This could mean that both elements were trapped in or car-
452 ried by the same species. Organic matter or sulfur containing species could originate

453 from biosolids recycled from wastewater treatment plants (WWTPs) and used as ferti-
454 lizers and soil amendments (Healy et al., 2016; Le Pape et al., 2012).



455

456 Figure 8. Number concentration of Ag-NPs as function as the concentration of total Sb in water samples from the agricultural water-
457 shed.

458 Several studies have confirmed the release of Ag-NPs in the effluent of WWTPs, at the
459 level from $< 12 \text{ ng L}^{-1}$ up to 100 ng L^{-1} (Li et al., 2013; Mitrano et al., 2012). . An his-
460 torical pollution for Sb and As as well as Ag is reported and well known in the Seine
461 river watershed (Ayrault et al., 2010; Le Cloarec et al., 2011). We cannot exclude this
462 old source that because of its dispersion via the atmosphere all over the catchment has
463 probably reached the agricultural watershed under investigation. Therefore, it suggests
464 that silver nanoparticles in agricultural water would be of anthropogenic origin.

465

466 In the case of urban river water samples, no clear correlations with the previously men-
467 tioned drivers such as organic matter or trace elements issued from anthropogenic activi-

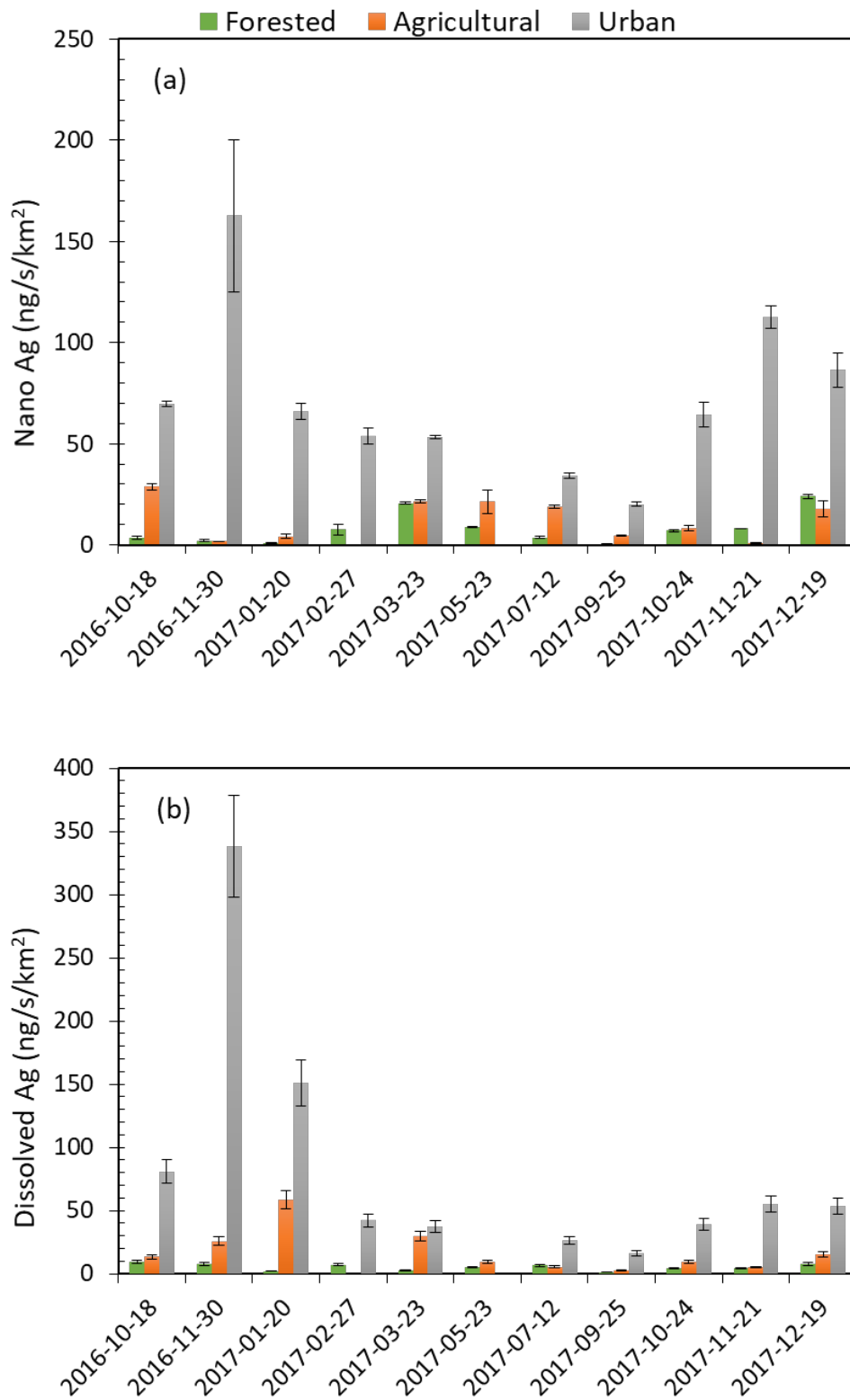
ities are reported. A recent evaluation on historical trace pollutants load (Sb, Ag, Ni, Cu, Zn, As, Pb) in the Seine River watershed reports lower values in sediments reflecting the progressive decontamination of the catchment (Le Gall et al., 2018). Thus new source of silver such as biocidal plastics and textiles (Vance, 2015) are uncorrelated to those historical trace pollutant elements as seen in this study. In addition, the mixed contribution of three type of waters (forested 19%, agricultural 44% and artificial 37%) makes complex the interpretation of the source identification especially in the case of small watersheds that promptly react to hydrological and environmental changes. A weak trend is observed between Ag-NPs number concentration and the temperature of the sampling river ($r^2 = 0.48$, $p = 0.0377$). The higher the temperature the higher the number of Ag-NPs. Temperature and sunlight, affects the reductive formation of Ag-NPs (Yin et al., 2014, 2012b). In summer, warmer water temperature months, increased exposition to UV-light would promote the reduction of Ag^+ by organic compounds leading to higher Ag-NPs concentrations (Badireddy et al., 2014; Odzak et al., 2017; Yin et al., 2015). Similar enhanced process by sunlight takes place for the reduction-formation Ag-NPs by natural EPS components (Kroll et al., 2014). They thus result in the persistence of Ag-NPs in sunlight waters.

The issue of the land-use effect is still standing even after identifying potential sources for the forested watershed samples (natural) and the agricultural watershed (contamination). Calculation of normalized fluxes of Ag-NPs that can be obtained by the combination of the monthly water discharge data and the respective area of the three watersheds may help to evidence clear differences between each of the studied sites.

490

491

492 **3.3 Effect of Land-use on exportation fluxes**



493

494 Figure 9. Export rate of nano (a) and dissolved (< 1 kDa) (b) Ag in three catchments throughout the sampling year. Error bars

495 represent the standard deviation of three measurements.

496

497

498 The measured normalized (in $\text{km}^{-2} \text{y}^{-1}$) export rate for Ag-NPs and dissolved silver are
499 given in Fig. 9. It is clear in this figure that the flux from the urban site is the highest for
500 nano and dissolved silver. If the monthly export rates of Ag-NPs are averaged, an annu-
501 al export rate of $2.3 \pm 1.3 \text{ g km}^{-2} \text{y}^{-1}$ is obtained. This value is ten times higher than the
502 export rate calculated for the agricultural and forested watersheds whose respective val-
503 ues are 0.4 ± 0.3 and $0.2 \pm 0.2 \text{ g km}^{-2} \text{y}^{-1}$. The difference between the urban site and the
504 two others is also seen for dissolved Ag export rates that are respectively equal to $2.6 \pm$
505 3.1 , 0.6 ± 0.5 and $0.2 \pm 0.1 \text{ g km}^{-2} \text{y}^{-1}$ for urban, agricultural and forested sites. These
506 large difference cannot be due to due to the constant release of Ag-NPs from consumer
507 products into freshwaters as reported in several studies, (Benn and Westerhoff, 2008;
508 Mitrano et al., 2014); (Farkas and Thomas, 2011); Aznar et al., 2017; Kaegi and
509 Burkhardt, 2010). The amount of nanosized silver registered in the R-nano French de-
510 claration of use or production site (<https://www.r-nano.fr/>) is equal to 10kg in 2017 and
511 was equal to 1 kg in 2013. In addition for France, in the
512 <https://www.nanotechproject.org/cpi/> data base of products with nano-sized silver, only
513 33 products are listed. Another approach is to use the data of Wang et al. (2018) for
514 Europe and downscale it to France, using Europe and France population as the scaling
515 factor, we can estimate that 27 kg Ag-Nano y^{-1} (i.e., $0.042 \text{ g km}^{-2} \text{y}^{-1}$) and 425 kg Ag-
516 Nano y^{-1} (i.e. $0.66 \text{ g km}^{-2} \text{y}^{-1}$) could be delivered to soils and waters, respectively. These
517 are very small numbers for the French territory. Other sources of Ag-NPs must be found
518 to account for the fluxes in all three watersheds. In table S4 we have compiled the
519 known input data of bulk Ag and Nano Ag to soils for the world, Europe, France and
520 Switzerland with available data from (Johnson et al., 2005; Muller and Novack, 2008
521 and Wang et al., 2018). We can clearly see that bulk Ag, issued mostly from WWTPs,
522 represents a much bigger source of Ag to soils and consequently to rivers or aquatic
523 ecosystems than the input of nano-Ag (Wang et al., 2018).

524 Material flow analysis, expressed in mass per capita per year or in mass per km² per
525 year, relies on land-use or product use to simulate concentrations of Ag-NPs in aquatic
526 systems. As two of the three watersheds are experiencing different land-uses (i.e., for-
527 forestry, agricultural practices and artificial areas), we can recalculate the actual specific
528 export rate of Ag-NPs for agricultural practices and artificial areas. The forested water-
529 shed ($0.2 \pm 0.2 \text{ g km}^{-2} \text{ y}^{-1}$ or $80 \text{ mg.capita}^{-1} \cdot \text{y}^{-1}$) is one end-member that will allow the
530 calculation of the agricultural end-member since the agricultural basin is only covered
531 by those two types of activities (i.e., 72% agriculture and 22% forestry). The calculated
532 rate of export of Ag-NPs is therefore equal to $0.5 \pm 0.3 \text{ g km}^{-2} \text{ y}^{-1}$ or $5 \text{ mg.capita}^{-1} \cdot \text{y}^{-1}$ for
533 land only used for agricultural purposes. Now the same calculation can be done for the
534 artificial areas using the urban watershed data (i.e., 37% artificial areas, 44% agriculture
535 19% forestry). The calculated rate of export of Ag-NPs is therefore equal to $5.5 \pm 3.0 \text{ g}$
536 $\text{km}^{-2} \text{ y}^{-1}$ or $3 \text{ mg.capita}^{-1} \cdot \text{y}^{-1}$ for artificial areas.

537 Considering the large uncertainties due to the high variability of Ag-NPs concentrations
538 along the year for artificial land and agricultural practices we can conclude that both
539 activities generate the same amounts of Ag-NPs expressed in $\text{mg.capita}^{-1} \cdot \text{y}^{-1}$, the highest
540 of all being the forested watershed (i.e. $80 \text{ mg.capita}^{-1} \cdot \text{y}^{-1}$ vs $5 \text{ mg.capita}^{-1} \cdot \text{y}^{-1}$). The ma-
541 jor characteristic of forested watershed is that its lithology corresponds to a sandy soil
542 vs. carbonated soils for the other watersheds and that it is richer in carbon in the top-soil
543 (Bonnot, 2015). Recent studies have shown that soils organic matter could significantly
544 contribute to the formation of silver nanoparticles in soils (Huang et al., 2019) . The low
545 number of inhabitants and the favored production of Ag-NPs by soils organic matter
546 would account for this higher number.

547 The origin of the Ag-NPs for the agricultural and urban watersheds is probably different
548 from the geochemical background and is from anthropogenic origin since in the Seine
549 river watershed, biosolids were and are used on agricultural land (Buzier et al., 2011;

550 Thévenot et al., 2007). Artificial areas will generate the highest flux of Ag-NPs by more
551 than one order of magnitude compared to the two other land uses when expressed in g
552 $\text{km}^{-2} \text{y}^{-1}$. The CORINE Land Cover Map (updated in 2006) can be used to calculate the
553 total Ag-NPs annual export for the entire catchment of the Seine River (i.e., 78650 km^2)
554 using two end-members. An urban one corresponding to 13% of the total catchment
555 (Ag-NPs = $5.5 \pm 3.0 \text{ g km}^{-2} \text{y}^{-1}$) and an average value corresponding to the agricultural
556 and forested end-members, which represents the rest of the land use in the catchment
557 (Ag-NPs = $0.4 \pm 0.3 \text{ g km}^{-2} \text{y}^{-1}$). The calculated flux is equal to $80 \pm 51 \text{ kg y}^{-1}$ corre-
558 sponding to a release per capita of $4 \text{ mg.capita}^{-1}.\text{y}^{-1}$. The urban source representing $56 \pm$
559 30 kgy^{-1} . The same calculation can be done for the dissolved fraction of Ag with the
560 same hypothesis. The dissolved flux of Ag is $94 \pm 50 \text{ kg y}^{-1}$ with the urban source repre-
561 senting $64 \pm 30 \text{ kg y}^{-1}$. In total a flux of 174 kg y^{-1} of silver would be exported from the
562 catchment dissolved and nano. This flux is much smaller than the particulate flux calcu-
563 lated by Ayrault equal to 1700 kgy^{-1} in 2003 (Ayrault et al., 2010) corresponding to a
564 flux of $85 \text{ mg.capita}^{-1}.\text{y}^{-1}$. Table S4 data show a huge input to soils of bulk silver in
565 France compared to the nano Silver (whatever the units used) and suggest that the dif-
566 ference between our seine river flux and the one from Ayrault et al., (2010) could be
567 due to a missing source input not captured by our 3 watersheds but existing at the scale
568 of the larger seine river watershed. For instance the cause could be higher inputs of
569 biosolids from WWTPs on agricultural land (Thevenot et al., 2007; Buzier et al., 2011)
570 since we do not have the mass of biosolids that are actually spread over the lands in our
571 three sites. In addition the data from Ayrault et al. (2010) was calculated with data from
572 sediments of two cores about 100 km downstream of Paris draining 96% of the Seine
573 River basin and are located within the last major meander of the Seine River before it
574 reaches its estuary. This location has been flooded at least once each year until 2004
575 (Ayrault et al., 2010). Flood events were never recorded in our small watersheds during

576 our year of survey and could explain part of the discrepancy as we are missing in our
577 calculations all the material arriving during the flood events. Thus despite the increased
578 use of Ag-NPs consumer products (Benn and Westerhoff, 2008; Farkas and Thomas,
579 2011; Kaegi and Burkhardt, 2010) their contribution to the general flow is still limited
580 (i.e., $\leq 7\%$ Table XX), more long term surveys are needed to confirm this result.”

581

582 **4. Conclusion**

583 Our results clearly demonstrate that material flow analysis models should generate ex-
584 port rates that are land-use dependent in order to have improved predicting capabilities.
585 Ag-NPs in three surface waters were found in the range of 1.5×10^7 to 2.3×10^9 particles
586 L^{-1} at number concentration and 0.4 to 28.3 $ng L^{-1}$ at mass concentration. In addition,
587 some driving process factors and potential sources were identified by using correlations
588 between Ag-NPs concentrations and other parameters, like the control of natural organic
589 matters of Ag-NPs in the forested water. Whereas, various contributions and more com-
590 plex process were found in agricultural and urban waters. Besides, the export rate of
591 Ag-NPs from artificial, agricultural and forested areas were respectively, 5.5 ± 3.0 , 0.5
592 ± 0.3 and $0.2 \pm 0.2 g km^{-2} y^{-1}$.

593 In addition, our study also demonstrates that the dissolved compartment should be taken
594 into account in material flow analysis and toxicity models since it is the most reactive as
595 well as the most toxic. Future studies should be focused on high resolution samplings
596 during a given specific month when climatic factor varies a lot and when farming and/or
597 hunting activities are active to better constrain the sources of the Ag-NPs as well as
598 their fluxes.

599

600 **Acknowledgment**

601 This project has been supported by Ile de France Region through the DIM Analytics
602 program (Convention ESPCI-RVT-IPGP-N°2015-3).

603 Part of this work was supported by grants from Région Ile-de-France R2DS and PIREN
604 Seine programs.

605 Parts of this work were supported by IPGP multidisciplinary program PARI, and by
606 Paris–IdF region SESAME Grant no. 12015908.

607 **References**

- 608 Aja, S.U., Wood, S.A., Williams-Jones, A.E., 1995. The aqueous geochemistry of Zr
609 and the solubility of some Zr-bearing minerals. *Appl. Geochemistry* 10, 603–620.
610 [https://doi.org/10.1016/0883-2927\(95\)00026-7](https://doi.org/10.1016/0883-2927(95)00026-7)
- 611 Akaighe, N., MacCuspie, R.I., Navarro, D.A., Aga, D.S., Banerjee, S., Sohn, M.,
612 Sharma, V.K., 2011. Humic Acid-Induced Silver Nanoparticle Formation Under
613 Environmentally Relevant Conditions. *Environ. Sci. Technol.* 45, 3895–3901.
614 <https://doi.org/10.1021/es103946g>
- 615 Ayrault, S., Priadi, C.R., Evrard, O., Lefèvre, I., Bonté, P., 2010. Silver and thallium
616 historical trends in the Seine River basin. *J. Environ. Monit.* 12, 2177–2185.
617 <https://doi.org/10.1039/c0em00153h>
- 618 Aznar, R., Barahona, F., Geiss, O., Ponti, J., José Luis, T., Barrero-Moreno, J., 2017.
619 Quantification and size characterisation of silver nanoparticles in environmental
620 aqueous samples and consumer products by single particle-ICPMS. *Talanta* 175,
621 200–208. <https://doi.org/10.1016/j.talanta.2017.07.048>
- 622 Badireddy, A.R., Farner Budariz, J., Marinakos, S.M., Chellam, S., Wiesner, M.R.,
623 2014. Formation of Silver Nanoparticles in Visible Light-Illuminated Waters:
624 Mechanism and Possible Impacts on the Persistence of AgNPs and Bacterial Lysis.
625 *Environ. Eng. Sci.* 31, 338–349. <https://doi.org/10.1089/ees.2013.0366>
- 626 Benedetti, M.F., Dia, A., Riotte, J., Chabaux, F., Gérard, M., Boulègue, J., Fritz, B.,
627 Chauvel, C., Bulourde, M., Déruelle, B., Ildefonse, P., 2003a. Chemical
628 weathering of basaltic lava flows undergoing extreme climatic conditions: The
629 water geochemistry record. *Chem. Geol.* 201, 1–17. [https://doi.org/10.1016/S0009-](https://doi.org/10.1016/S0009-2541(03)00231-6)
630 [2541\(03\)00231-6](https://doi.org/10.1016/S0009-2541(03)00231-6)
- 631 Benedetti, M.F., Mounier, S., Filizola, N., Benaim, J., Seyler, P., 2003b. Carbon and
632 metal concentrations, size distributions and fluxes in major rivers of the Amazon

633 basin. *Hydrol. Process.* 17, 1363–1377. <https://doi.org/10.1002/hyp.1289>

634 Benn, T.M., Westerhoff, P., 2008. Nanoparticle silver released into water from
635 commercially available sock fabrics. *Environ. Sci. Technol.* 42, 4133–4139.
636 <https://doi.org/10.1021/es7032718>

637 Bian, Y., Kim, K., Ngo, T., Kim, I., Bae, O.N., Lim, K.M., Chung, J.H., 2019. Silver
638 nanoparticles promote procoagulant activity of red blood cells: A potential risk of
639 thrombosis in susceptible population. *Part. Fibre Toxicol.* 16.
640 <https://doi.org/10.1186/s12989-019-0292-6>

641 Bonnot, C., 2015. L'origine des métaux et la dynamique du zinc dans le bassin de la
642 Seine.

643 Bonnot, C.A., Gélabert, A., Louvat, P., Morin, G., Proux, O., Benedetti, M.F., 2016.
644 Trace metals dynamics under contrasted land uses: contribution of statistical,
645 isotopic, and EXAFS approaches. *Environ. Sci. Pollut. Res.* 1–21.
646 <https://doi.org/10.1007/s11356-016-6901-0>

647 Boxall, A., Chaudhry, Q., Sinclair, C., Jones, A., Aitken, R., Jefferson, B., Watts, C.,
648 2007. Current and future predicted environmental exposure to engineered
649 nanoparticles, Environment. Central Science Laboratory, York, UK.
650 <https://doi.org/196111>

651 Buzier, R., Tusseau-Vuillemin, M.H., Keirsbulck, M., Mouchel, J.M., 2011. Inputs of
652 total and labile trace metals from wastewater treatment plants effluents to the Seine
653 River. *Phys. Chem. Earth* 36, 500–505. <https://doi.org/10.1016/j.pce.2008.09.003>

654 Chen, J. Bin, Gaillardet, J., Bouchez, J., Louvat, P., Wang, Y.N., 2014. Anthropophile
655 elements in river sediments: Overview from the Seine River, France.
656 *Geochemistry, Geophys. Geosystems* 15, 4526–4546.
657 <https://doi.org/10.1002/2014GC005516>

658 Cornelis, G., Hasselöv, M., 2014. A signal deconvolution method to discriminate

659 smaller nanoparticles in single particle ICP-MS. *J. Anal. At. Spectrom.* 29, 134–
660 144. <https://doi.org/10.1039/c3ja50160d>

661 Del Real, A.E.P., Castillo-Michel, H., Kaegi, R., Sinnet, B., Magnin, V., Findling, N.,
662 Villanova, J., Carrière, M., Santaella, C., Fernández-Martínez, A., Levard, C.,
663 Sarret, G., 2016. Fate of Ag-NPs in Sewage Sludge after Application on
664 Agricultural Soils. *Environ. Sci. Technol.* 50, 1759–1768.
665 <https://doi.org/10.1021/acs.est.5b04550>

666 Delay, M., Dolt, T., Woellhaf, A., Sembritzki, R., Frimmel, F.H., 2011. Interactions and
667 stability of silver nanoparticles in the aqueous phase: Influence of natural organic
668 matter (NOM) and ionic strength. *J. Chromatogr. A* 1218, 4206–4212.
669 <https://doi.org/10.1016/j.chroma.2011.02.074>

670 Desmau, M., Gélabert, A., Levard, C., Ona-Nguema, G., Vidal, V., Stubbs, J.E., Eng,
671 P.J., Benedetti, M.F., 2018. Dynamics of silver nanoparticles at the
672 solution/biofilm/mineral interface. *Environ. Sci. Nano.*
673 <https://doi.org/10.1039/C8EN00331A>

674 Dobrzyńska, M.M., Kruszewski, M., 2014. Genotoxicity of silver and titanium dioxide
675 nanoparticles in bone marrow cells of rats in vivo. *Toxicology* 315, 86–91.
676 <https://doi.org/10.1016/j.tox.2013.11.012>

677 Dumont, E., Johnson, A.C., Keller, V.D.J., Williams, R.J., 2015. Nano silver and nano
678 zinc-oxide in surface waters – Exposure estimation for Europe at high spatial and
679 temporal resolution. *Environ. Pollut.* 196, 341–349.
680 <https://doi.org/10.1016/j.envpol.2014.10.022>

681 Dumont, E., Williams, R.J., 2015. Nano silver and nano zinc-oxide in surface waters –
682 Exposure estimation for Europe at high spatial and temporal resolution. *Environ.*
683 *Pollut.* 196, 341–349. <https://doi.org/10.1016/j.envpol.2014.10.022>

684 Estebe, A., Mouchel, J.M. Thevenot, D.R., 1998. Urban Runoff impacts on Particulate

685 Metal Concentrations. *Water. Air. Soil Pollut.* 108, 83–50.
686 <https://doi.org/10.1023/A:1005064307862>

687 Estèbe, A., Boudries, H., Mouchel, J.M., Thévenot, D.R., 1997. Urban runoff impacts
688 on particulate metal and hydrocarbon concentrations in river Seine: Suspended
689 solid and sediment transport. *Water Sci. Technol.* 36, 185–193.
690 [https://doi.org/10.1016/S0273-1223\(97\)00600-8](https://doi.org/10.1016/S0273-1223(97)00600-8)

691 Farkas, J., Thomas, K.V., 2011. Characterization of the effluent from a nanosilver
692 producing washing machine. *Environ. Int.* 37, 1057–1062.
693 <https://doi.org/10.1016/j.envint.2011.03.006>

694 Gaillet, S., Rouanet, J.M., 2015. Silver nanoparticles: Their potential toxic effects after
695 oral exposure and underlying mechanisms - A review. *Food Chem. Toxicol.*
696 <https://doi.org/10.1016/j.fct.2014.12.019>

697 Garban B, Ollivon D, Carru AM, C.A., 1996. Origin, retention and release of trace
698 metals from sediments of the river seine 87, 363–381.

699 Good, K.D., Bergman, L.E., Klara, S.S., Leitch, M.E., VanBriesen, J.M., 2016.
700 Implications of engineered nanomaterials in drinking water sources. *J. Am. Water*
701 *Works Assoc.* 108, E1–E17. <https://doi.org/10.5942/jawwa.2016.108.0013>

702 Gottschalk, F., Lassen, C., Nowack, B., 2015. Modeling flows and concentrations of
703 nine engineered nanomaterials in the Danish environment. *Int. J. Environ. Res.*
704 *Public Health* 12, 5581–5602. <https://doi.org/10.3390/ijerph120505581>

705 Grosbois, C., Meybeck, M., Horowitz, A., Ficht, A., 2006. The spatial and temporal
706 trends of Cd, Cu, Hg, Pb and Zn in Seine River floodplain deposits (1994-2000).
707 *Sci. Total Environ.* 356, 22–37. <https://doi.org/10.1016/j.scitotenv.2005.01.049>

708 Guo, L., Santschi, P.H., 2007. Ultrafiltration and its Applications to Sampling and
709 Characterisation of Aquatic Colloids. *Environ. Colloids Part.*, Wiley Online Books.
710 <https://doi.org/doi:10.1002/9780470024539.ch4>

711 Healy, M.G., Fenton, O., Forrestal, P.J., Danaher, M., Brennan, R.B., Morrison, L.,
712 2016. Metal concentrations in lime stabilised, thermally dried and anaerobically
713 digested sewage sludges. *Waste Manag.* 48, 404–408.
714 <https://doi.org/10.1016/j.wasman.2015.11.028>

715 Hodson, M.E., 2002. Experimental evidence for mobility of Zr and other trace elements
716 in soils. *Geochim. Cosmochim. Acta* 66, 819–828. [https://doi.org/10.1016/S0016-](https://doi.org/10.1016/S0016-7037(01)00803-1)
717 [7037\(01\)00803-1](https://doi.org/10.1016/S0016-7037(01)00803-1)

718 Horowitz, A.J., Meybeck, M., Idlafkih, Z., Biger, E., 1999. Variations in trace element
719 geochemistry in the Seine River Basin based on floodplain deposits and bed
720 sediments. *Hydrol. Process.* 13, 1329–1340. [https://doi.org/10.1002/\(SICI\)1099-](https://doi.org/10.1002/(SICI)1099-1085(19990630)13:9<1329::AID-HYP811>3.0.CO;2-H)
721 [1085\(19990630\)13:9<1329::AID-HYP811>3.0.CO;2-H](https://doi.org/10.1002/(SICI)1099-1085(19990630)13:9<1329::AID-HYP811>3.0.CO;2-H)

722 Huang, Y.-N., Qian, T.-T., Dang, F., Yin, Y.-G., Li, M., Zhou, D.-M., 2019. Significant
723 contribution of metastable particulate organic matter to natural formation of silver
724 nanoparticles in soils. *Nat. Commun.* 10, 4–11. [https://doi.org/10.1038/s41467-](https://doi.org/10.1038/s41467-019-11643-6)
725 [019-11643-6](https://doi.org/10.1038/s41467-019-11643-6)

726 Ilina, S.M., Lapitskiy, S.A., Alekhin, Y. V., Viers, J., Benedetti, M., Pokrovsky, O.S.,
727 2016. Speciation, Size Fractionation and Transport of Trace Elements in the
728 Continuum Soil Water–Mire–Humic Lake–River–Large Oligotrophic Lake of a
729 Subarctic Watershed. *Aquat. Geochemistry* 22, 65–95.
730 <https://doi.org/10.1007/s10498-015-9277-8>

731 Johnston, H.J., Hutchison, G., Christensen, F.M., Peters, S., Hankin, S., Stone, V., 2010.
732 A review of the in vivo and in vitro toxicity of silver and gold particulates: Particle
733 attributes and biological mechanisms responsible for the observed toxicity. *Crit.*
734 *Rev. Toxicol.* 40, 328–346. <https://doi.org/10.3109/10408440903453074>

735 Kaegi, R., Burkhardt, M., 2010. Release of silver nanoparticles from outdoor facades.
736 *Environ. Pollut.* 158, 2900–2905. <https://doi.org/10.1016/j.envpol.2010.06.009>

737 Klaus, T., Joerger, R., Olsson, E., Granqvist, C.-G., 1999. Silver-based crystalline
738 nanoparticles, microbially fabricated. *Proc. Natl. Acad. Sci.* 96, 13611–13614.
739 <https://doi.org/10.1073/pnas.96.24.13611>

740 Kroll, A., Behra, R., Kaegi, R., Sigg, L., 2014. Extracellular polymeric substances
741 (EPS) of freshwater biofilms stabilize and modify CeO₂ and Ag nanoparticles.
742 *PLoS One* 9. <https://doi.org/10.1371/journal.pone.0110709>

743 Labille, J., Harns, C., Bottero, J.-Y., Brant, J., 2015. Heteroaggregation of titanium
744 dioxide nanoparticles with natural clay colloids. *Environ. Sci. Technol.* 49, 6608–
745 6616. <https://doi.org/10.1021/acs.est.5b00357>

746 Lambert, T., Bouillon, S., Darchambeau, F., Morana, C., Roland, F.A.E., Descy, J.P.,
747 Borges, A. V., 2017. Effects of human land use on the terrestrial and aquatic
748 sources of fluvial organic matter in a temperate river basin (The Meuse River,
749 Belgium). *Biogeochemistry* 136, 191–211. [https://doi.org/10.1007/s10533-017-](https://doi.org/10.1007/s10533-017-0387-9)
750 [0387-9](https://doi.org/10.1007/s10533-017-0387-9)

751 Le Cloarec, M.F., Bonte, P.H., Lestel, L., Lefèvre, I., Ayrault, S., 2011. Sedimentary
752 record of metal contamination in the Seine River during the last century. *Phys.*
753 *Chem. Earth* 36, 515–529. <https://doi.org/10.1016/j.pce.2009.02.003>

754 Le Gall, M., Ayrault, S., Evrard, O., Laceby, J.P., Gateuille, D., Lefèvre, I., Mouchel,
755 J.M., Meybeck, M., 2018. Investigating the metal contamination of sediment
756 transported by the 2016 Seine River flood (Paris, France). *Environ. Pollut.* 240,
757 125–139. <https://doi.org/10.1016/j.envpol.2018.04.082>

758 Le Pape, P., Ayrault, S., Quantin, C., 2012. Trace element behavior and partition versus
759 urbanization gradient in an urban river (Orge River, France). *J. Hydrol.* 472–473,
760 99–110. <https://doi.org/10.1016/j.jhydrol.2012.09.042>

761 Lea, M.C., 1889. On allotropic forms of silver. *Am. J. Sci.* s3-38, 476–491.
762 <https://doi.org/10.2475/ajs.s3-38.223.47>

763 Levard, C., Reinsch, B.C., Michel, F.M., Oumahi, C., Lowry, G. V., Brown, G.E., 2011.
764 Sulfidation processes of PVP-coated silver nanoparticles in aqueous solution:
765 Impact on dissolution rate. *Environ. Sci. Technol.* 45, 5260–5266.
766 <https://doi.org/10.1021/es2007758>

767 Li, C.C., Wang, Y.J., Dang, F., Zhou, D.M., 2016. Mechanistic understanding of
768 reduced AgNP phytotoxicity induced by extracellular polymeric substances. *J.*
769 *Hazard. Mater.* 308, 21–28. <https://doi.org/10.1016/j.jhazmat.2016.01.036>

770 Li, L., Hartmann, G., Döblinger, M., Schuster, M., 2013. Quantification of nanoscale
771 silver particles removal and release from municipal wastewater treatment plants in
772 Germany. *Environ. Sci. Technol.* 47, 7317–7323.
773 <https://doi.org/10.1021/es3041658>

774 Lu, Q., He, Z.L., Stoffella, P.J., 2012. Land application of biosolids in the USA: A
775 review. *Appl. Environ. Soil Sci.* <https://doi.org/10.1155/2012/201462>

776 Mitrano, D.M., Leshner, E.K., Bednar, A., Monserud, J., Higgins, C.P., Ranville, J.F.,
777 2012. Detecting nanoparticulate silver using single-particle inductively coupled
778 plasma-mass spectrometry. *Environ. Toxicol. Chem.* 31, 115–121.
779 <https://doi.org/10.1002/etc.719>

780 Mitrano, D.M., Rimmele, E., Wichser, A., Erni, R., Height, M., Nowack, B., 2014.
781 Presence of nanoparticles in wash water from conventional silver and nano-silver
782 textiles. *ACS Nano* 8, 7208–7219. <https://doi.org/10.1021/nn502228w>

783 Montaña, M.D., Badiei, H.R., Bazargan, S., Ranville, J.F., 2014. Improvements in the
784 detection and characterization of engineered nanoparticles using spICP-MS with
785 microsecond dwell times. *Environ. Sci. Nano* 1, 338–346.
786 <https://doi.org/10.1039/c4en00058g>

787 Mueller, N.C., Nowack, B., 2008. Exposure modelling of engineered nanoparticles in
788 the environment. *Environ. Sci. Technol.* 42, 44447–53.

789 <https://doi.org/10.1021/es7029637>

790 Musee, N., 2010. Simulated environmental risk estimation of engineered nanomaterials:
791 A case of cosmetics in Johannesburg City. *Hum. Exp. Toxicol.* 30, 1181–1195.
792 <https://doi.org/10.1177/0960327110391387>

793 Nowack, B., Krug, H.F., Height, M., 2011. 120 years of nanosilver history: Implications
794 for policy makers. *Environ. Sci. Technol.* 45, 1177–1183.
795 <https://doi.org/10.1021/es103316q>

796 O'Brien, N., Cummins, E., 2010. Nano-scale pollutants: Fate in Irish surface and
797 drinking water regulatory systems. *Hum. Ecol. Risk Assess.* 16, 847–872.
798 <https://doi.org/10.1080/10807039.2010.501270>

799 Odzak, N., Kistler, D., Sigg, L., 2017. Influence of daylight on the fate of silver and
800 zinc oxide nanoparticles in natural aquatic environments. *Environ. Pollut.* 226, 1–
801 11. <https://doi.org/10.1016/j.envpol.2017.04.006>

802 Pace, H.E., Rogers, N.J., Jarolimek, C., Coleman, V.A., Gray, E.P., Higgins, C.P.,
803 Ranville, J.F., 2012. Single particle inductively coupled plasma-mass
804 spectrometry: a performance evaluation and method comparison in the
805 determination of nanoparticle size. *Environ. Sci. Technol.* 46, 12272–80.
806 <https://doi.org/10.1021/es301787d>

807 Pace, H.E., Rogers, N.J., Jarolimek, C., Coleman, V.A., Higgins, C.P., Ranville, James
808 F.Pace, H.E., 2011. Determining Transport Efficiency for the Purpose of Counting
809 and Sizing Nanoparticles via Single Particle Inductively Coupled Plasma Mass
810 Spectrometry. *Anal. Chem.* 83, 9361–9369. <https://doi.org/10.1021/ac300942m>

811 Peters, R.J.B., van Bommel, G., Milani, N.B.L., den Hertog, G.C.T., Undas, A.K., van
812 der Lee, M., Bouwmeester, H., 2018. Detection of nanoparticles in Dutch surface
813 waters. *Sci. Total Environ.* 621, 210–218.
814 <https://doi.org/10.1016/j.scitotenv.2017.11.238>

815 Qi, H., Hu, R., Zhang, Q., 2007. Concentration and distribution of trace elements in
816 lignite from the Shengli Coalfield, Inner Mongolia, China: Implications on origin
817 of the associated Wulantuga Germanium Deposit. *Int. J. Coal Geol.* 71, 129–152.
818 <https://doi.org/10.1016/j.coal.2006.08.005>

819 Reimann, C., Fabian, K., Birke, M., Filzmoser, P., Demetriades, A., Négrel, P., Oorts,
820 K., Matschullat, J., de Caritat, P., Albanese, S., Anderson, M., Baritz, R., Batista,
821 M.J., Bel-Ian, A., Cicchella, D., De Vivo, B., De Vos, W., Dinelli, E., Ďuriš, M.,
822 Dusza-Dobek, A., Eggen, O.A., Eklund, M., Ernsten, V., Flight, D.M.A., Forrester,
823 S., Fügedi, U., Gilucis, A., Gosar, M., Gregorauskiene, V., De Groot, W., Gulan,
824 A., Halamić, J., Haslinger, E., Hayoz, P., Hoogewerff, J., Hrvatovic, H., Husnjak,
825 S., Jähne-Klingberg, F., Janik, L., Jordan, G., Kaminari, M., Kirby, J., Klos, V.,
826 Kwećko, P., Kuti, L., Ladenberger, A., Lima, A., Locutura, J., Lucivjansky, P.,
827 Mann, A., Mackovych, D., McLaughlin, M., Malyuk, B.I., Maquil, R., Meuli,
828 R.G., Mol, G., O'Connor, P., Ottesen, R.T., Pasniecna, A., Petersell, V.,
829 Pflleiderer, S., Poňavič, M., Prazeres, C., Radusinović, S., Rauch, U., Salpeteur, I.,
830 Scanlon, R., Schedl, A., Scheib, A., Schoeters, I., Šefčik, P., Sellersjö, E.,
831 Slaninka, I., Soriano-Disla, J.M., Šorša, A., Svrkota, R., Stafilov, T., Tarvainen, T.,
832 Tendavilov, V., Valera, P., Verougstraete, V., Vidojević, D., Zissimos, A.,
833 Zomeni, Z., Sadeghi, M., 2018. GEMAS: Establishing geochemical background
834 and threshold for 53 chemical elements in European agricultural soil. *Appl.*
835 *Geochemistry* 88, 302–318. <https://doi.org/10.1016/j.apgeochem.2017.01.021>

836 Sal'nikov, D.S., Pogorelova, A.S., Makarov, S. V, Vashurina, I.Y., 2009. Silver ion
837 reduction with peat fulvic acids. *Russ. J. Appl. Chem.* 82, 545–548.
838 <https://doi.org/10.1134/S107042720904003X>

839 Shevlin, D., O'Brien, N., Cummins, E., 2018. Silver engineered nanoparticles in
840 freshwater systems – Likely fate and behaviour through natural attenuation

841 processes. *Sci. Total Environ.* 621, 1033–1046.
842 <https://doi.org/10.1016/j.scitotenv.2017.10.123>

843 Silva, B.F. da, Pérez, S., Gardinalli, P., Singhal, R.K., Mozeto, A.A., Barceló, D., 2011.
844 Analytical chemistry of metallic nanoparticles in natural environments. *TrAC -*
845 *Trends Anal. Chem.* <https://doi.org/10.1016/j.trac.2011.01.008>

846 Sonke, J.E., 2006. Lanthanide–Humic Substances Complexation. II. Calibration of
847 Humic Ion-Binding Model V. *Environ. Sci. Technol.* 40, 7481–7487.

848 Sun, T.Y., Bornhöft, N.A., Hungerbühler, K., Nowack, B., 2016. Dynamic Probabilistic
849 Modeling of Environmental Emissions of Engineered Nanomaterials. *Environ. Sci.*
850 *Technol.* 50, 4701–4711. <https://doi.org/10.1021/acs.est.5b05828>

851 Tharaud, M., Gardoll, S., Khelifi, O., Benedetti, M.F., Sivry, Y., 2015. UFREASI:
852 User-FRiendly Elemental dAta procesSIng. A free and easy-to-use tool for
853 elemental data treatment. *Microchem. J.* 121, 32–40.
854 <https://doi.org/10.1016/j.microc.2015.01.011>

855 Tharaud, M., Gondikas, A.P., Benedetti, M.F., von der Kammer, F., Hofmann, T.,
856 Cornelis, G., 2017. TiO₂ nanomaterial detection in calcium rich matrices by
857 spICPMS. A matter of resolution and treatment. *J. Anal. At. Spectrom.* 32, 1400–
858 1411. <https://doi.org/10.1039/C7JA00060J>

859 Thévenot, D.R., Moilleron, R., Lestel, L., Gromaire, M.C., Rocher, V., Cambier, P.,
860 Bonté, P., Colin, J.L., de Pontevès, C., Meybeck, M., 2007. Critical budget of
861 metal sources and pathways in the Seine River basin (1994-2003) for Cd, Cr, Cu,
862 Hg, Ni, Pb and Zn. *Sci. Total Environ.* 375, 180–203.
863 <https://doi.org/10.1016/j.scitotenv.2006.12.008>

864 Topuz, E., Sigg, L., Talinli, I., 2014. A systematic evaluation of agglomeration of Ag
865 and TiO₂nanoparticles under freshwater relevant conditions. *Environ. Pollut.* 193,
866 37–44. <https://doi.org/10.1016/j.envpol.2014.05.029>

867 Topuz, E., Talinli, I., 2015. Agglomeration of Ag and TiO₂nanoparticles in surface and
868 wastewater: Role of calcium ions and of organic carbon fractions. *Environ. Pollut.*
869 204, 313–323. <https://doi.org/10.1016/j.envpol.2015.05.034>

870 Tuoriniemi, J., Hassellöv, M., 2012. Size discrimination and detection capabilities of
871 single-particle ICPMS for environmental analysis of silver nanoparticles. *Anal.*
872 *Chem.* 84, 3965–3972. <https://doi.org/10.1021/ac203005r>

873 Vance, M.E., 2015. Nanotechnology in the real world: Redeveloping the nanomaterial
874 consumer products inventory. *Beilstein J. Nanotechnol.* 6, 1769–1780.
875 <https://doi.org/10.3762/bjnano.6.181>

876 Verwijmeren, J., Wiering, M.A., 2007. Many rivers to cross. Cross border co-operation
877 in river management, *Transport Reviews - TRANSP REV.*

878 Wang, P., Lombi, E., Menzies, N.W., Zhao, F.J., Kopittke, P.M., 2018. Engineered
879 silver nanoparticles in terrestrial environments: a meta-analysis shows that the
880 overall environmental risk is small. *Environ. Sci. Nano* 5, 2531–2544.
881 <https://doi.org/10.1039/C8EN00486B>

882 Wen, L.S., Santschi, P.H., Gill, G.A., Paternostro, C.L., Lehman, R.D., 1997. Colloidal
883 and particulate silver in river and estuarine waters of Texas. *Environ. Sci. Technol.*
884 31, 723–731. <https://doi.org/10.1021/es9603057>

885 Wimmer, A., Kalinnik, A., Schuster, M., 2018. New insights into the formation of
886 silver-based nanoparticles under natural and semi-natural conditions. *Water Res.*
887 141, 227–234. <https://doi.org/10.1016/j.watres.2018.05.015>

888 Yang, X., Lin, S., Wiesner, M.R., 2014. Influence of natural organic matter on transport
889 and retention of polymer coated silver nanoparticles in porous media. *J. Hazard.*
890 *Mater.* 264, 161–168. <https://doi.org/10.1016/j.jhazmat.2013.11.025>

891 Yang, Y., Wang, Q., 2016. Analysis of silver and gold nanoparticles in environmental
892 water using single particle-inductively coupled plasma-mass spectrometry. *Sci.*

893 Total Environ. Yang) 563564, 996–1007.
894 <https://doi.org/10.1016/j.scitotenv.2015.12.150>

895 Yin, Y., Liu, J., Jiang, G., 2012a. Sunlight-Induced Reduction of Ionic Ag and Au to
896 Metallic Nanoparticles by Dissolved Organic Matter. ACS Nano 6, 7910–7919.
897 <https://doi.org/10.1021/nn302293r>

898 Yin, Y., Liu, J., Jiang, G., 2012b. Sunlight-induced reduction of ionic Ag and Au to
899 metallic nanoparticles by dissolved organic matter. ACS Nano 6, 7910–7919.
900 <https://doi.org/10.1021/nn302293r>

901 Yin, Y., Shen, M., Zhou, X., Yu, S., Chao, J., Liu, J., Jiang, G., 2014. Photoreduction
902 and stabilization capability of molecular weight fractionated natural organic matter
903 in transformation of silver ion to metallic nanoparticle. Environ. Sci. Technol. 48,
904 9366–9373. <https://doi.org/10.1021/es502025e>

905 Yin, Y., Yang, X., Zhou, X., Wang, W., Yu, S., Liu, J., Jiang, G., 2015. Water
906 chemistry controlled aggregation and photo-transformation of silver nanoparticles
907 in environmental waters. J. Environ. Sci. (China) 34, 116–125.
908 <https://doi.org/10.1016/j.jes.2015.04.005>

909 Yu, S., Liu, J., Yin, Y., Shen, M., 2018. Interactions between engineered nanoparticles
910 and dissolved organic matter: A review on mechanisms and environmental effects.
911 J. Environ. Sci. (China) 63, 198–217. <https://doi.org/10.1016/j.jes.2017.06.021>

912 Zhang, T., Jiang, G., 2017. Role of Secondary Particle Formation in the Persistence of
913 Silver Nanoparticles in Humic Acid Containing Water under Light Irradiation.
914 Environ. Sci. Technol. 51, 14164–14172. <https://doi.org/10.1021/acs.est.7b04115>
915

Electronic Supplementary Material (for online publication only)

[Click here to download Electronic Supplementary Material \(for online publication only\): Supplementary materials V3.0.docx](#)